https://doi.org/10.5194/gmd-2022-143
Preprint. Discussion started: 26 July 2022

Geoscientific Model Development Discussions

PVN 1.0: using dynamic PFTs and restoration scenarios to model CO2 and CH4 emissions in peatlands

Tanya J.R. Lippmann[1], Monique M.P.D. Heijmans[2], Han Dolman[3,4], Ype van der Velde[1], Dimmie M.D. Hendriks[5], and Ko van Huissteden[1,6]

[1]Vrije Universiteit Amsterdam, Amsterdam, the Netherlands
[2]Wageningen University and Research, Wageningen, the Netherlands
[3]Royal Netherlands Institute for Sea Research, Texel, the Netherlands
[4]Netherlands Earth System Science Center, Utrecht, the Netherlands
[5]Deltares Research Institute, Utrecht, the Netherlands
[6]VOF Kytalyk Carbon Cycle Research, Utrecht, the Netherlands

Correspondence: Tanya J.R. Lippmann (t.j.r.lippmann@vu.nl)

Abstract. Peatlands are the world's largest terrestrial carbon store. Despite covering only 3% of the planet's land surface, peatlands store 30% of the planet's terrestrially available carbon. The Dutch government's 2019 National Climate Agreement committed to reduce the contribution of peatlands to total national Dutch GHG emissions, by 1 $\mathrm{MtonCO_2}$ per year (or 20%) until 2030. Countries with similarly degraded peatlands are likely to face similar commitments in the coming years. Restoration (or rewetting) is a proposed solution to reduce land subsidence and increase carbon sequestration in agricultural peatlands but is often accompanied by large CH_4 emissions.

Whilst, previous studies have investigated whether singular plant types impact the greenhouse gas (GHG) emissions of peatlands, few (or no) studies have investigated the impact of plant composition on GHG emissions in peatlands. To assess the impact of dynamic vegetation on subsequent GHG fluxes in peatlands, we developed a new model, Peatland-VU-NUCOM (PVN). This is the second process-based model to date, capable of simulating dynamic vegetation, CO_2, and CH_4 emissions in peatlands.

The new PVN model simulates CH_4 and CO_2 fluxes in relation to the plant community composition. The PVN model includes plant competition, CH_4 diffusion, ebullition, root, shoot, litter exudate production, belowground decomposition, and aboveground moss development, under changing water table and climatic conditions. The model was compared against observational data collected at two sites in the Netherlands.

These results showed that plant communities impact net GHG emissions. This is the first time that a peatland emissions model is able to investigate the role of re-introducing peat forming vegetation on subsequent GHG emissions. We also found that the initial plant community influenced the potential for harvest events to reduce GHG emissions. These results indicated that plant community restoration is a critical component of peatland restoration.

https://doi.org/10.5194/gmd-2022-143
Preprint. Discussion started: 26 July 2022

Geoscientific Model Development Discussions

1 Introduction

Peatlands are the world's largest terrestrial carbon store. Despite covering only 3% of the planet's land surface, peatlands store 30% or 644 GtC of the planet's terrestrially available carbon (Yu et al., 2010). Whilst, the present day radiative effect of peatlands on the climate is estimated to be between -0.2 and -0.5 Wm^{-2} (i.e. a net cooling) (Frolking and Roulet, 2007), future changes to the climate will impact peat development and the carbon sequestration capacity of peatlands (Loisel et al., 2021). Peatlands are frequently subjected to burning or drainage for agricultural purposes which results in large amounts of lost C. Global peatland CO_2 emissions due to drainage increased by more than 20% in less than 30 years, from 1.06 to 1.3 $\mathrm{PgCO_2yr}^{-1}$ between 1990 and 2006 (Joosten, 2010).

Warming due to climate change is expected to be greatest at high latitudes, and has already begun (Doblas-Reyes et al., 2021). The net global effect of climate change on peatlands is not yet understood (Loisel et al., 2021). On the one hand, warmer soil temperatures are likely to lead to increased microbial and aerobic peat decomposition, leading to larger CO_2 and CH_4 emissions (Dorrepaal et al., 2009). However, wetter conditions in a warmer world may lead to peat development, and enhanced carbon sequestration (Lafleur et al., 2003). It appears likely that some peatlands will form a positive feedback (evidenced by Dorrepaal et al. (2009)), whist others will form a neutral (Saleska et al., 2002), or negative feedback to warming of the global climate system (Melillo et al., 2002) and the net effect of these complex responses is not yet known.

Peatlands (and other wetlands) are large natural sources of global atmospheric CH_4 (Spahni et al., 2011). Methane is the third most prevalent atmospheric greenhouse gas (GHG) and was estimated to contribute 30% of the total radiative forcing of CO_2 between 2005 and 2008 (Doblas-Reyes et al., 2021). Present day natural CH_4 emissions are 50% of total CH_4 emissions (Saunois et al., 2020). Natural CH_4 emissions, particularly wetlands, are the greatest source of uncertainty in the global methane budget (Saunois et al., 2020) and there exists a need to better constrain this estimate, requiring a better understanding of small scale peatland CH_4 processes (Bridgham et al., 2013).

The Dutch government's 2019 National Climate Agreement committed to reduce the contribution of peatlands to the total national Dutch GHG emissions, by 1 $\mathrm{MtonCO_2}$ per year (or 20%) until 2030 (et al. Van Der Ree, 2019). In the Netherlands, drainage of peatlands for agricultural purposes began approximately 2,000 years ago, resulting in 0.83 Gton C lost over the last thousand years (Erkens et al., 2016). 1.03 Gton of soil C is estimated to remain in peat stocks. The agricultural and economic benefits of peatland-based agriculture must be considered alongside the impacts on climate change and the natural values of peatlands (Bustamante et al., 2014). Strategies to reduce further carbon loss are being investigated (et al. Van Der Ree, 2019).

Rewetting refers to the practice of re-raising surface water levels of drained peatlands with the aim to a) reduce land subsidence, b) facilitate land-use alternatives, or c) enhance ecosystem services (Knox et al., 2015). Field studies haved shown that rewetted peatlands are accompanied by enhanced CH_4 and net GHG emissions, sometimes persisting for decades (Harpenslager et al., 2015; Knox et al., 2015). Ecosystem restoration and carbon sequestration are critical steps to mitigating anthropogenic climate change (IPCC Working Group II, 2022).

Models are a necessary tool to analyse the long-term impacts of changing environmental drivers on ecosystems. Many peatland carbon cycle models have been developed over the preceding decades. The Wetland and Wetland CH_4 Intercomparison

https://doi.org/10.5194/gmd-2022-143
Preprint. Discussion started: 26 July 2022


Geoscientific Model Development Discussions

of Models Project (WETCHIMP) evaluated the ability of a variety of models to simulate large-scale wetland characteristics and corresponding CH_4 emissions (Melton et al., 2013; Wania et al., 2013). Previous modelling efforts that have investigated the potential of rewetted drained peatlands to reduce global radiative forcing Günther et al. (2020), have ignored the presence of enhanced CH_4 emissions subsequent to rewetting.

The inclusion of vegetation classes is critical for modelling C and CH_4 storage and emissions in peatlands (Li et al., 2016). Plant growth, root exudation and decomposition of organic matter (OM) occur to differing extents and happen at different rates depending on the plant type (Dorrepaal et al., 2007). Ecosystem storage of carbon happens through CO_2 uptake by photosynthesis and the slow decomposition of plant matter, leaf and root detritus, and root exudates in the anaerobic zone. Plant detritus and root exudates excretion play a critical role in the availability of carbonic compounds and these vary depending on plant type. This means that shifts in community composition lead to feedbacks between species and other environmental parameters such as soil moisture, bulk density, soil organic matter (SOM) content, gas conduit function, rate of growth, rate of decomposition, microbial mineralisation, aerobic decomposition (De Boeck et al., 2011). Dynamic plant representation are critical for the model's ability to reproduce and assess environmental feedbacks (Toet et al., 2006).

To fully understand the role of vegetation emissions feedbacks during peatland restoration efforts, plants must be treated as a dynamic interactive element of the peatland ecosystem. Peatland modelling efforts have worked to address the difficulty of reliably simulating CH_4 fluxes in peatlands, by either focusing on CO_2 or surface water levels as the primary indicator of carbon exchange and the net greenhouse gas flux (Metzger et al., 2015).

Plant functional types (PFTs) allow functions and structures to be grouped among plants (Wullschleger et al., 2014). Dynamic (rather than static) PFTs are critical to reliably assess the impacts of anthropogenic climate change on peatland ecosystems (Box et al., 2019). The functionality and scope of current peatland models that include (dynamic or static) PFTs are compared in Table 1. PEATBOG is the singular preceding peatland model that includes vegetation dynamics, CO_2, and CH_4 cycling (Wu and Blodau, 2013). There is an urgent need to expand model development efforts that assess the role of vegetation emissions feedbacks during and subsequent to peatland restoration efforts, which requires the inclusion of dynamic PFTs within peatland emission models.

Plot scale models are a necessary tool for understanding peatland dynamics because the small-sale heterogeneity in peatland topography (e.g. the pervasive formation of hummocks and hollows in ombotrophic peatlands) impacts GHG emissions on the scale of 1-10 metres (Gorham, 1991). Whilst, gridded peatland models, such as PEATBOG, have the advantage of representing regional and global scales (Wania et al., 2013), the heterogenous nature of peatlands means that plot and landscape scale models are a necessary tool for those managing peatland landscapes (such as farmers, nature conservation institutions, and stakeholders) to make informed assessments that relate climatic changes, ecosystem functioning, and agricultural practices.

To investigate the impact of peatland restoration methods, we assess the impact of dynamic vegetation classes on subsequent GHG fluxes in peatlands, we develop a new model, Peatland-VU-NUCOM (PVN 1.0). PVN 1.0 incorporates features of NUCOM-BOG (an ecosystem competition plot-scale model (Heijmans and Berendse, 2008) into PVN, a new version of Peatland-VU (a peatland process-based plot-scale model (van Huissteden et al., 2006). This study investigates two peat restoration pathways, abandonment and re-establishment. The first pathway, rewetting followed by abandonment, refers to rewetting

https://doi.org/10.5194/gmd-2022-143
Preprint. Discussion started: 26 July 2022


Geoscientific Model Development Discussions

activities that do not consider vegetation restoration. The second pathway, rewetting followed by re-establishment, refers to
90 rewetting activities that re-establish, or re-introduce, peat forming vegetation. We hypothesise that plant composition influences the GHG emissions subsequent rewetting. Automated flux-chamber measurements taken at two peatland sites, one 'abandoned' and one 're-established' site, in the Netherlands are used to evaluate the model. The new PVN model simulates CH_4 and CO_2 fluxes in relation to the plant community composition, including the belowground and decomposition of plant detritus under changing water table and climatic conditions.

https://doi.org/10.5194/gmd-2022-143
Preprint. Discussion started: 26 July 2022

Geoscientific Model Development Discussions

Table 1. Range and scope of current peatland models using PFTs. We've only counted the number of peatland specific PFTs. Some models use more PFTs than what have been counted here.

Model	Gridded	Site specific	Timestep	PFTs	Competition	CO_2	CH_4	Citation
PEATBOG	Y	Y	daily	3	Y	Y	Y	Wu et al. (2016)
LPJ-WHyMe v1.3.1	Y	N	daily, yearly	2	Y	Y	Y	Wania et al. (2010)
MILENNIA	N	Y	annual, century	8	N	Y	Y	Heinemeyer et al. (2010)
$CH4MOD_{wetland}$	N	Y	daily	4	N	N	Y	Li et al. (2016)
McGill Wetland Model	N	Y	daily	4	N	Y	N	Wu et al. (2011)
Holocene Peat Model	N	Y	annual	12	Y	N	N	Frolking et al. (2010)
CLASS3.6–CTEM2.0	Y	N	daily	4	N	Y	N	Wu et al. (2016)
ORCHIDEE-PEAT	Y	Y	daily	1	N	Y	N	Largeron et al. (2018); Krinner et al. (2005); Ringeval et al. (2010)
LPJ-GUESS	Y	Y	yearly	5	Y	Y	N	Smith et al. (2001); Chaudhary et al. (2017)
Bauer	N	Y	yearly	4	N	Y	N	Bauer (2004)
LPJ-WHy v1.2	Y	N	monthly	2	Y	N	N	Wania et al. (2009)
GUESS-ROMUL	Y	N	daily	1	N	N	N	Yurova et al. (2007)
DYPTOP	Y	Y	monthly	4	N	N	N	Stocker et al. (2014)
LPX-Bern DGVM v1.4	Y	N	millennial	5	Y	N	N	Müller and Joos (2020)
Community Land Model 4.5	Y	Y	6 hr	4	N	N	N	Shi et al. (2015)
CaMP v2.0	N	Y	annual	Y	N	Y	Y	Bona et al. (2020)
NUCOM	N	Y	monthly	5	Y	Y	N	Heijmans et al. (2008)
PEATLAND	N	Y	daily	-	N	Y	Y	van Huissteden et al. (2006)
PVN	N	Y	daily	unlimited	Y	Y	Y	this publication

2 Materials and Methods

The PVN model describes the vegetation, carbon, water, CH_4 and CO_2 dynamics of an undisturbed, disturbed or rewetted column of an above- and below-ground peatland ecosystem in a temperate to sub-boreal climate. PVN 1.0 incorporates features

https://doi.org/10.5194/gmd-2022-143
Preprint. Discussion started: 26 July 2022


Geoscientific Model Development Discussions

of the NUCOM-BOG into PVN, a new version of the Peatland-VU model. NUCOM-BOG simulates vegetation competition, C, nutrient, and water cycling in undisturbed bog ecosystems under changing climates. A full description of the model can be found in Heijmans and Berendse (2008). NUCOM-BOG simulates a water table and a soil profile divided by the acrotelm-catotelm boundary. Plant growth and decomposition is partitioned between plant organs. The Peatland-VU model simulates the CH_4 and CO_2 fluxes of a column of peat soil with a varying water table. A full description of the model can be found in van Huissteden et al. (2006, 2009). Peatland-VU incorporates adapted versions of modules that simulate CH_4 fluxes (Mi et al., 2014; Walter et al., 2001), gross primary productivity & photosynthesis (Haxeltine et al., 1996; Sitch et al., 2003) whilst assuming a constant plant layer and does not include a nitrogen cycle. The ecosystem in PVN represents a square meter column that stretches above- and below-ground. Carbon dioxide and CH_4 emissions enter the atmosphere by ebullition, transport through plants, diffusion through the soil, and respiration. Figure 1 shows a schematic, detailing the CO_2 and CH_4 pools and processes of the new PVN model.

In this part of the paper, we start by describing the two sites that are being simulated (Sect. 2.1). We then describe the inclusion of PFTs in PVN (Sect. 2.1.1). This is followed by an outline of the model processes, in the order that they are executed by the model (Sect. 2.2). These processes are displayed in the model schematic in Fig. 1 and extensive descriptions of the original NUCOM and Peatand-VU can models can be found in Heijmans and Berendse (2008); van Huissteden et al. (2006), respectively. We then explain the model optimization process using site-based field measurements of vegetation composition, CO_2 and CH_4 fluxes (Sect. 2.2.1). We used in situ meteorological climate data and regional hydrological model output as input data (Sect. 2.3). We then describe the field data collected to evaluate the model's ability to reproduce observed fluxes (Sect. 2.4). Finally, we describe the six restoration scenarios and the methodology used to compare different model scenarios (Sect. 2.5).

2.1 Simulating two restored sites

This study simulated two degraded peatland sites in North Holland, the Netherlands (locations shown in Fig. 2); the Horstermeer (52°15' N, 5°04' E; 2.1 metres below sea level (mbsl)) and the Ilperveld (52°26' N, 4°56' E; 1.42 mbsl). The Horstermeer site is a former agricultural peat meadow where use was ceased in the 1990s and the water table was also raised. Horstermeer is now a semi-natural meadow containing very heterogenous vegetation, including reeds, grasses, and small shrubs, and is not subject to mowing or other forms of land management (Hendriks et al., 2007). Horstermeer was a freshwater lake that was drained as part of large-scale land reclamation project completed in 1888. Until the 1990s, it was used for grazing and therefore exposed to manure fertilisation.

The Ilperveld site is a former raised bog complex that was drained to be used as agricultural pasture, and was frequently exposed to manure fertilisation (van Geel et al., 1983; Harpenslager et al., 2015). Ilperveld is currently a nature recreation area. The site is mown twice a year, in June and September. Since the early 2000's, the Ilperveld has undergone restoration efforts which include raising the water level, attempts to re-introduce *Sphagnum*, and water quality management. Vegetation profiles show layers of intact *Sphagnum*/*Carex* peat and unlike intact peatlands, the top layer has undergone greater decomposition due to land management since drainage (Harpenslager et al., 2015).

https://doi.org/10.5194/gmd-2022-143
Preprint. Discussion started: 26 July 2022

Geoscientific Model Development Discussions

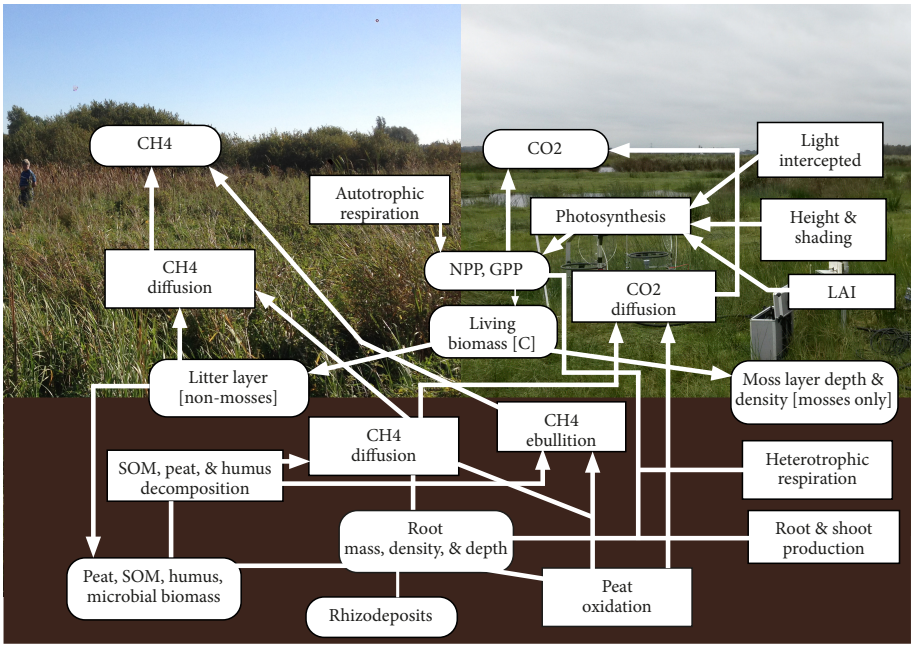

Figure 1. Schematic of the production, consumption and transport of carbon in the model. Dynamics and processes are dilineated with rectangles, whereas carbon pools are dilineated with curved edges.

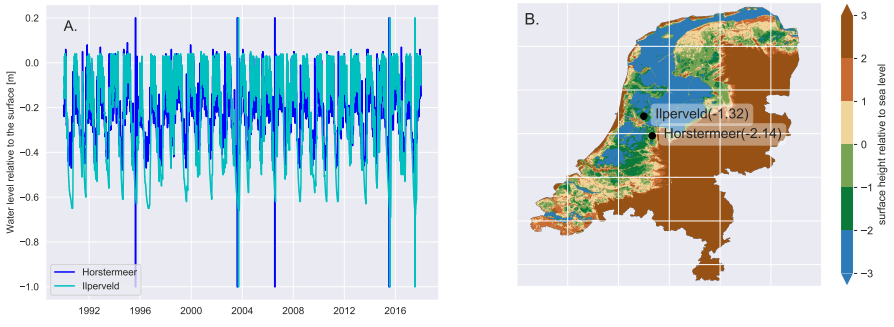

Figure 2. A. The location of the 2 field sites and the land surface height in the Netherlands and B. The water table heights relative to the land surface over the simulated period, 1990-2018. These AHN land surface heights were used to localise the NHI 250mx250m surface water levels.

2.1.1 New PFT parametrisation

Vegetation in the model is described in terms of the fractional coverage of each PFT. Any number of PFTs can be included in the model simulation. This study defined 6 PFTs (*Typha*, sedges, tall grasses, short grasses, *Sphagnum*, brown mosses) based on the vegetation communities observed at the Horstermeer and Ilperveld sites. Each PFT has prescribed ideal and

https://doi.org/10.5194/gmd-2022-143
Preprint. Discussion started: 26 July 2022


Geoscientific Model Development Discussions

tolerated temperature and water table limits that impact above and belowground production. Some PFT attributes describe plant physiology, whilst others reflect dynamics or bioclimatic limits. PFT parameters and assocaited values are listed in Table Fig. S1. Plant traits were amalgamated from the NUCOM-bog model, the TRY 5.0 database (https://www.try-db.org, last accessed 18 May 2022) (Kattge et al., 2011, 2020) and other relevant publications listed in table Fig. S3. Each PFT is prescribed minimum and maximum ideal and tolerated temperatures, and water table depths for growth. Each PFT is prescribed either evergreen or deciduous phenology. For deciduous plants, leaf senescence occurs when daily temperatures fall below minimum tolerated temperatures. Maximum leaf coverage is maintained so long as daily water depth and temperature are within the ideal threshold.

The sum of all PFTs are constrained to a maximum value of 100%. Cover fraction (CF) is calculated monthly, based on the ratio of PFT biomass to total biomass (Eq. 1). All PFTs have a minimum CF of 0.1% and are able to further establish when the conditions become favourable, as in NUCOM.

$$CF_{t,p} = \frac{CB_{t,p}}{\sum_{p=1}^{n}(CB_{t,p})} \tag{1}$$

where, CB = biomass (Ckg), t refers to time, and p refers to PFT.

2.2 Model processes

In the initialisation scheme, the multiple carbon pools are initialised. This includes the below ground roots, shoots, and exudates; belowground CO_2 and CH_4 pools; peat and SOM. Aboveground, the LB, litter layer, and moss depth is initialised. These carbon pools are initialised for each PFT based on prescribed CF and C:biomass ratios. The soil profile can comprise any number of soil horizons of unequal thicknesses, defined in a site specific soil profile, which the model converts internally to layers of equal thickness, as in Peatland-VU. This study divides the soil profile into 15 soil layers, each 10 cm thick, for both sites.

Above- and below- ground biomass pools are initialised according to the specified CF and C:biomass ratio for each PFT. To account for differences in decomposition rates among roots, shoots and exudates, each PFT has designated pools of roots, shoots, exudates, SOM, and microbial biomass reservoirs. Moss PFTs have shoots, belowground biomass (SOM), & microbial biomass, contribute to the belowground peat pool but do not have roots whilst, non-moss PFTs have belowground SOM reservoirs but do not contribute to the peat pool. Root distribution (RD), and root mass (Eq. 2) decrease exponentially from the surface to the PFT maximum root depth.

New roots are calculated based on a (prescribed) shoot growth factor and primary production (calculated daily). Root exudates (Eq. 3) and shoots are a parameterised mass fraction of calculated belowground root production. Root mass (RM), distribution (RD), root growth and die off are calculated daily for each PFT. Released carbon due to root senescence and exudation is partitioned between soil carbon reservoirs.

$$RM(PFT,t,z) = RM_{p,t-1,z} \cdot RD_{p,z,t} - REX_{p,t} - RDR_{p,t} \tag{2}$$

https://doi.org/10.5194/gmd-2022-143
Preprint. Discussion started: 26 July 2022


Geoscientific Model Development Discussions

where,

$$REX = RD_{p,t,z} \cdot FSP_{p,DoY} \cdot REX_{p,t} \tag{3}$$

where, DoY represents the day of the year, REX represents the root exudate factor so that maximum exudates occurs during spring ($FSP_{p,DoY}$) and,

$$RDR_{p,t} = RM_{p,t,z} \cdot RSX_p \tag{4}$$

where RDR represents the amount of dead roots, calculated using root senescence rate, RSX.

Belowground SOM is partitioned between active and inert. PFTs are prescribed different levels of microbial activity. Active carbon is available for microbial decomposition and then partitioned between CO_2 and CH_4. MOSS PFTs contribute to the belowground peat pool and do not have a surface litter layer. Instead, dead plant material is added directly to the belowground pools. Height is calculated as a function of biomass and shading impacts the effective incoming solar radiation.

Incoming solar radiation is calculated (as described in PV van Huissteden et al. (2006)) above the canopy at the start of each day. Then, Leaf Area Index (LAI) is calculated as a function of LB, water growth factor, the LAI of the previous day, as well as the SLA and LEC whilst, constrained by prescribed maximum and minimum LAI values. Light not absorbed by non-moss PFTs, reaches is distributed between the moss PFTs, proportional to their CF.

$$LAI_{t,p} = \frac{CB_{t,p} \cdot SLA_p}{(LEC_p \cdot LAI_{t-1,p} + (1 - e^{-f_{W,t,p}}))} \tag{5}$$

where SLA = Specific Leaf Area, LEC = Light Extension Coefficient, W refers to water depth.

PFT height is calculated by an allometric relation to Cbiomass, as a function of time, per PFT (Huang et al., 1992; Smith et al., 2001):

$$H_{t,p} = k_1 \cdot D_{t,p}^{k_2} \tag{6}$$

where,

$$D_{t,p} = \left(\frac{4 \cdot CB_{t,p}}{WD \cdot \pi \cdot k_2} \right)^{\frac{1}{2+k_3}} \tag{7}$$

where, WD, k_1, k_2, and k_3 are constants.

All non-moss PFTs are ordered according to descending height. The fraction of light received by the plant after shading (i.e. light interception) is calculated (Eq. 8). The remaining LI, is shared between the moss PFTs. Light interception (LI) is used to determine the amounts of effective incoming radiation and photosynthesis, and aboveground respiration for each plant.

$$LI_{t,non-moss} = (1 - e^{-LEC_p}) \cdot CB_{t,p} \cdot SLA_p \tag{8}$$

Potential growth is calculated for each PFT (Eq. 9), and is a function of LI, ideal and extreme atmospheric CO_2, temperature and water table limits, incorporated from Heijmans and Berendse (2008). Potential Growth is impacted if water table depth or temperature fall within tolerated bounds but outside of the ideal threshold.

$$PG_{t,p} = LI_{p,t} \cdot Gmax_p \cdot KCO2_{t,p} \cdot f_{T,t,p} \cdot f_{W,t,p} \tag{9}$$

https://doi.org/10.5194/gmd-2022-143
Preprint. Discussion started: 26 July 2022


Geoscientific Model Development Discussions

where, LI = Light Intercepted, $Gmax$ = maximum growth rate, T refers to temperature.

C3 Photosynthesis, net primary productivity (NPP), and plant respiration are calculated daily using a modified version of the photosynthesis scheme from Peatland-VU. The adapted photosynthesis function uses LI and the minimum and maximum temperature limits prescribed per PFT. Therefore, shading by taller plants impacts photosynthesis and respiration, for each PFT. Photosynthesis, respiration, and NPP are summed across the PFTs at the end of each day.

Senescence is calculated for the aboveground LB and added to the litter layer (for non-moss PFTs). Part of the litter layer is added to the belowground SOM pool. The harvest scheme is activated, if prescribed in the model input files. Root senescence and exudation occur contributing to belowground CO_2 and CH_4. Aerobic decomposition of inert belowground SOM contribute to CO_2 production. Methane fluxes (ebullition, oxidation, plant transport) are calculated per PFT and plant transport is dependent on plant growth limits. A portion of CH_4 is oxidised to CO_2 per PFT. At the end of each month, the CF and moss thickness schemes are activated. Ecosystem carbon, biomass and SOM pools are aggregated at the end of each timestep.

The harvest height and days are optional prescribed model parameters. This is a similar approach to the periodic harvest scheme used in land surface model, JULES-BE (Littleton et al., 2020) and an adapted form of the harvest function in Peatland-VU. PFTs taller than the prescribed height are harvested. During a simulated harvest event, 20% of harvested material remains uncollected in the field and is added to the litter layer. Living biomass is decreased by the proportional biomass lost, under the assumption that biomass is uniformly distributed with height. Lastly, LAI is recalculated.

The depth (or thickness) of the living moss layer is calculated monthly and dependent on CB, dry bulk density (DBD), and CF. PFT moss thicknesses are aggregated for ecosystem moss depth (MHG):

$$MHG = \frac{SHG_{t,p}}{\sum_{PFT=1}^{n} CF_{t,p}} \tag{10}$$

where,

$$SHG_{t,p} = \sum_{PFT=1}^{n} (HG_{t,p} \cdot CF_{t,p}) \tag{11}$$

$$HG_{t,p} = \frac{PG_{t,p} \cdot CF_{t,p}}{DBD_{t,p,z=1}} \tag{12}$$

where, MD = moss depth, PG = potential growth, DBD = dry bulk density.

The belowground SOM pools are divided partitioned between the soil layers. A portion of the SOM pool is decomposed each day and the result is partitioned into CO_2, microbial biomass, resistant OM, and humus, where, the daily accumulation of microbial biomass and humus stores are also subject to daily decomposition.

$$\frac{\delta Q}{\delta t} = k \cdot Q \tag{13}$$

where Q is the mass of organic C in a specific SOM pool per unit volume of soil ($\mathrm{kgm^{-3}}$). k is the decomposition rate constant ($\mathrm{day^{-1}}$) applied to each SOM pool, calculated for microbial biomass and humus.

$$KCO2_{t,p} = 1 - (kH_{t,p} + kM_{t,p}) \cdot \frac{\delta Q}{\delta t} \tag{14}$$

https://doi.org/10.5194/gmd-2022-143
Preprint. Discussion started: 26 July 2022


Geoscientific Model Development Discussions

where, $KCO2$ represents the flux rate of CO_2 , kh the amount of available humus, and kM the amount of available microbial biomass.

Methane fluxes (ebullition (Qeb), oxidation (Rox), plant transport (Qpl)) are calculated per PFT. Where, plant transport is dependent on ideal and tolerated plant growth limits (calculated by PG in Eq. 9). The net CH_4 flux depends on CH_4 production in the anaerobic soil zone, consumption by methanotrophic bacteria in the aerobic zone and transport pathways to the atmosphere (van Huissteden et al., 2006; Mi et al., 2014; Walter and Heimann, 2000). Microbial activity is dependent on both prescribed PFT microbial activity and ecosystem $Q10$ values.

$$\frac{\delta}{\delta t} DCH_{4t,z,p} = -\frac{\delta}{\delta Z} Fdiff_{t,z,p} + Qeb_{t,z,p} + Qpr_{t,z,p} + Rpr_{t,z,p} + Rox_{t,z,p} \tag{15}$$

where D_{CH_4} is the CH_4 concentration $Fdiff$ is the diffusive flux. Rpr and Rox represent CH_4 production and oxidation (Eq. 16), respectively. Methane oxidation is temperature sensitive and is dependent on the CH_4 concentration at each time step (Eq. 16). Qox determines the temperature sensitivity of the process and is PFT specific. Rox represents the contribution of soil oxidation to CH_4

$$Rox_{t,p} = -\frac{V_{max} CH_{4_{t,z,p}}}{Km + CH4_t, z, p} \cdot Qox_p^{\frac{T(t,z)-T_{ref}}{10}} \tag{16}$$

where, where Km (μM) and $Vmax$ (μM h^{-1}) are Michaelis–Menten constants. Rpr represents the CH_4 production:

$$Rpr_{p,z} = R0_p \cdot Cl_{p,z} \cdot Q10_p^{\frac{T_{t,z}-T_{ref}}{10}} \tag{17}$$

where, $R0$ is a constant rate factor (μMH^{-1}), Cl is the amount of available labile C, and T_{ref} is the soil reference temperature. where, the plant transport (Qpl) is calculated by:

$$Qpl_{t,z,p} = -cP_p \cdot vP_p \cdot RD_{z,p} \cdot PG_{t,p} \cdot DCH_{4_{t,z,p}} \tag{18}$$

where, cP and vP represent vegetation rate constants.

All model code has been written in C++. The model code is publicly available from the Bitbucket repository (bitbucket.org/tlippmann/pvn_public, last accessed 18 May 2022) under the GNU General Public License version 3, or any later version. Users are welcome to contact the authors for technical support.

2.2.1 Model calibration

The model was calibrated to match observational in situ chamber measurements, not previously published. A monte carlo analysis was used to calibrate the model input parameters. Since the size of the living, and decomposing carbon pools both above and below ground drive the CH_4 scheme, we first ensured that the photosynthesis, and above and below ground growth and respiration corresponded to observed CO_2 fluxes (NEE). Then, the CH_4 scheme was calibrated to agree with observational in situ chamber measurements, seperately for the 2 sites. Even though the amount of photosynthesis and LB does not directly impact the CH_4 production, which primarily occurs in the soil and aboveground litter layers, these processes are precursors to root and shoot growth, respiration, and senescence. After optimisation of the CH_4 fluxes, the non-observational based plant

https://doi.org/10.5194/gmd-2022-143
Preprint. Discussion started: 26 July 2022


Geoscientific Model Development Discussions

parameters were adjusted to bring the PFT CF in line with observed CF ratios (not previously published). The chosen PFT parameters influence the amount of litter produced, the below ground OM reservoirs, as well as the amount of photosynthesis, and LB. As well as there being additional parameters used by PVN, parameters used by PVN calibration differed from Peatland-VU. Attempts to run the old version of the model with new calibrated parameters did not yield results in the same order of magnitude as the observations. Therefore, it was necessary to use different model parameterisations for PVN and Peatland-VU.

2.3 Input data

Daily temperature, precipitation, evapotranspiration, and radiation data, measured at Schiphol, the nearest KNMI weather station were used as climate input (accessed via https://www.knmi.nl/nederland-nu/klimatologie/daggegevens, last accessed 18 May 2022) (figures in Fig. S1). The annual average rainfall was 850 mm over the period, 1990-2020, with approximately 1/3 (30%) of the rainfall falling in summer and autumn, respectively, and less than 1/4 (24%) falling in winter, with the remainder falling in the spring. The average daily temperature between 1990 and 2019 was 9.4 °Cand warmed approximately +0.1 $^{\circ}\mathrm{C yr}^{-1}$over the same period. The average daily temperature for the warmest month, August, was 22.1 °Cand the lowest daily monthly temperature for the coldest month, January, was 0.8 °C. The PVN model is site specific and therefore requires soil input data. This data was collected in 2015 and 2016 and includes DBD, C content, OM content, sand and clay content, pF curve. Soil profile data from the Horstermeer and Ilperveld field sites were used to build two soil parameter files. Water level input was sourced from the Dutch hydrological model, Netherlands Hydrological Instrument (NHI) (De Lange et al., 2014). NHI water level (mbsl) output was converted to relative surface height using the digital elevation map, Actueel Hoogtebestand Nederland (Alhoz et al., 2020). This conversion was computed using Python package, NumPy and plotted using Matplotlib (Fig. 2).

Initial input parameters of the model that were not observational measurements (climate, plant, water table), parameters are the outcome of either previous simulations, monte carlo caibration, or via expert judgement. In some ways, the model is somewhat initialised from a 'cold start'. For example, there is no CH_4 or CO_2 gas in the soil pore spaces. However, for other variables, the model begins in an 'equilibrated' state, as is the case of soil parameters such as DBD, SOM content, pH, C:N ratio, where the model variables are pre-set to the values that reflect the moment prior to the beginning of a simulation.

2.4 Evaluating simulated CO_2 and CH_4 fluxes

Flux data was collected between 2015 and 2017, aligned with standardised chamber technique measurement protocol (Pavelka et al., 2018). Carbon dioxide and CH_4 fluxes were measured using automated flux chambers (AC) and the Los Gatos Gas Analyser between 2015 and 2017 using 2-4 chambers per site. Chambers were made of transparent plastic, equipped with a fan and installed in the field using collars. Measurements were recorded 24 $\mathrm{hr day}^{-1}$ for a week at a time, upon which the AC system was moved to another site. We note that these observational datasets do not offer complete temporal continuity. The CO_2 and CH_4 concentrations were measured inside the chamber, whilst the chamber was closed, during 15 minute intervals. From this data, the daily hourly average CO_2 (net ecosystem exchange (NEE)) and CH_4 fluxes were calculated. To evaluate the

https://doi.org/10.5194/gmd-2022-143
Preprint. Discussion started: 26 July 2022


Geoscientific Model Development Discussions

model, we compared simulated and observed daily hourly average CO_2 and CH_4 fluxes. To indicate the degree of uncertainty, daily standard deviations were derived using the hourly fluxes.

2.5 Restoration scenarios

This study investigates 8 model scenarios that are summarised in Table 2. Two different plant compositions, (MOSS and TYPHA) are used across the Horstermeer and Ilperveld sites (HORST and ILP), and with harvests (H) and without harvests (NH). The MOSS (TYPHA) PFT composition is representative of the plants observed at the Ilperveld (Horstermeer). HORST_NH and ILP_H simulate the current situations at the Horstermeer and Ilperveld sites, respectively.

To investigate alternative plant compositions, we swapped the plant composition of both sites, rather than composing fictional community compositions. We aimed to maintain a sense of realism by using existing ecosystem plant compositions from a nearby peatland site. HORST_MOSS_NH and HORST_MOSS_H simulate the Horstermeer site (maintaining the same soil profile, WT input, and model calibration) using MOSS PFTs (short grass, tall grass, brown moss, and *Sphagnum*). ILP_TYPHA_H and ILP_TYPHA_NH simulate the Ilperveld site (maintaining the same soil profile, WT input, and model calibration) using TYPHA PFTs (*Typha*, sedges, short grass, tall grass).

In order to enable unbiased subtraction of relative differences between theoretica model scenarios and the current situation model scenarios, we calculated the log relative difference as

$$\text{log relative difference} = \ln \frac{x}{x_{ref}} \tag{19}$$

where, x represents the theoretical model result, and x_{ref} represent the reference model results, the HORST_NH and ILP_H scenarios. Törnqvist et al. (1985) demonstrated this alterntive for the ordinary relative difference ($x - x_{ref}/x_{ref}$). The log relative difference has symmetric, additive, normed properties, whereas, the ordinary relative differences range from -1 to infinity which, is an assymetric result that also has a positive bias, in the case of addition or subtraction.

The values for all GHG emissions are expressed as CO_2 equivalents ($\mathrm{kgCO_{2e}m^{-2}yr^{-1}}$) and calculated as

$$GHG_{CO_2e} = CH_4 \cdot GWP + CO_2 \tag{20}$$

where,

GWP_{20} = 83.6, as 1 $\mathrm{kgCH_4}$ = 83.6 kg CO_2e, over a 20 year time horizon, and

GWP_{100} = 25.0, as 1 $\mathrm{kgCH_4}$ = 25.0 kg CO_2e, over a 100 year time horizon (Solomon et al., 2007).

https://doi.org/10.5194/gmd-2022-143
Preprint. Discussion started: 26 July 2022

Geoscientific Model Development Discussions

Table 2. Description of simulations

Simulation Name	Vegetation	Harvest	Soil Profile	WT Input	Climate Input
HORST_NH	*Typha*, Sedges, short grass, tall grass	No	Horstermeer	Horstermeer	Schiphol
HORST_H	*Typha*, Sedges, short grass, tall grass	Yes	Horstermeer	Horstermeer	Schiphol
HORST_MOSS_NH	Short grass, tall grass, brown moss, *Sphagnum*	No	Horstermeer	Horstermeer	Schiphol
HORST_MOSS_H	Short grass, tall grass, brown moss, *Sphagnum*	Yes	Horstermeer	Horstermeer	Schiphol
ILP_H	Short grass, tall grass, brown moss, *Sphagnum*	Yes	Ilperveld	Ilperveld	Schiphol
ILP_NH	Short grass, tall grass, brown moss, *Sphagnum*	No	Ilperveld	Ilperveld	Schiphol
ILP_TYPHA_H	*Typha*, Sedges, short grass, tall grass	Yes	Ilperveld	Ilperveld	Schiphol
ILP_TYPHA_NH	*Typha*, Sedges, short grass, tall grass	No	Ilperveld	Ilperveld	Schiphol
PV_HORST_NH	N/A	No	Horstermeer	Horstermeer	Schiphol
PV_ILP_H	N/A	Yes	Ilperveld	Ilperveld	Schiphol

3 Results

We assess the role of including dynamic PFTs in a peatland emisions model. We ran the model using the multiple PFT-harvest-site scenarios described in table 2. First, we discuss observed daily O_2 (NEE) & CH_4flux measurements and plant CFs against simulated results, using time series and 1:1 plots. Next, we compare the results of the current-situation scenarios against two different peatland restoration efforts, re-establishment and abandonment over a 30 year period. Then we discuss the role of harvest on plant competition and GHG emissions. All model assessments began in 1995, following a 5 year spin-up period (1990-94, inclusive). An overview of the model scenarios assessed in this study are provided in Table 2. All net GHG values are expressed as CO_2 equivalents (CO_{2e}) and calculated using 20 (100) year GWPs using equation (20)).

3.1 Carbon dioxide and CH_4 fluxes reproduced at both sites

For assessment against observational data we compare observed flux measurements against simulated results using time series and 1:1 plots for CO_2 (Fig. 3), and CH_4 (Fig. 4) fluxes. Model-observation comparisons have been shown for days where observational data exists due to gaps in observational data. The daily flux uncertainty of the observations (black lines) increased during the summer months (JJA) during both measurement years, at both sites, for both CO_2 and CH_4, (Fig. 3) & CH_4 (Fig. 4), respectively. We have confidence that the model reproduces results within the spread of the uncertainity of the observations at both sites.

3.1.1 CO_2 (NEE) fluxes are reproduced at both sites

The model (HORST_NH) reproduced the mean and SD of observed daily CO_2 fluxes at the Horstermeer (Fig. 3). PVN did not capture the magnitude of the CO_2 drawdown that occurs in April 2017 but reproduced the timing of the increasing CO_2

https://doi.org/10.5194/gmd-2022-143
Preprint. Discussion started: 26 July 2022

Geoscientific Model Development Discussions
Open Access
EGU

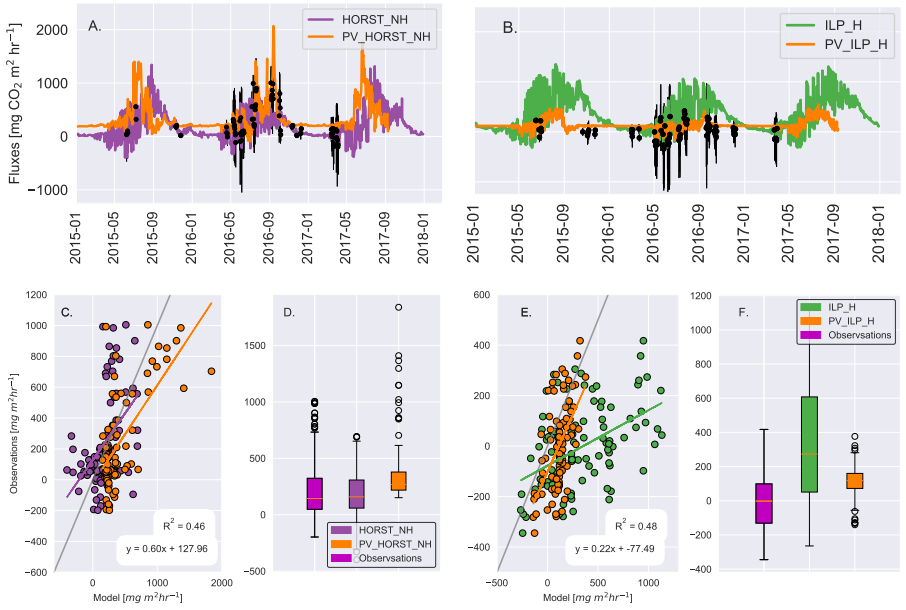

Figure 3. Simulated and observed carbon dioxide fluxes (NEE) at the Horstermeer (left) and Ilperveld (right). The black dots are in-situ flux chamber observational measurements in panels A & B. The 1:1 line is plotted in grey. The line of the linear regression and the R^2 correlation values are provided for comparison between PVN (HORST_NH & ILP_H) and the observations. Note the differing x and y axes.

fluxes during Spring from April to August in 2015 and 2016 and captured that decreasing observed fluxes that occur from September to December in 2015 and 2016. The occurrence of extreme (maximum and minimum) fluxes are similar, though slightly lesser for both maximum and minimum fluxes, compared to the observations. The PVN model resuts estimated that the 2015-17 annually averaged CO_2 emissions were 1.73 $\mathrm{kgCO_2m^{-2}yr^{-1}}$(HORST_NH), similar to the 1995-2017 annually averaged emissions, 1.65 $\mathrm{kgCO_2m^{-2}yr^{-1}}$. PVN generally estimated lower annual CO2 emissions than Peatland-VU. The Peatland-VU model (PV_HORST) estimated that both the 2015-17 and the 1995-2017 annually averaged emissions higher than HORST_NH, 2.74 $\mathrm{kgCO_2m^{-2}yr^{-1}}$and 2.81 $\mathrm{kgCO_2m^{-2}yr^{-1}}$, respectively.

HORST_NH estimated that the maximum annual CO_2 emissions occurred in 2014 (2.29 $\mathrm{kgCO_2m^{-2}yr^{-1}}$), whereas PV_HORST estimated the maximum annual emissions (4.38 $\mathrm{kgCO_2m^{-2}yr^{-1}}$) occurred in 1995. Thereby, HORST_NH estimated the maximum annual emissions occurred much more recently than PV_HORST. HORST_NH estimated that to the minimum annual emissions (1.12 $\mathrm{kgCO_2m^{-2}yr^{-1}}$) occurred in 1996, compared to the minimum annual emissions (1.81 $\mathrm{kgCO_2m^{-2}yr^{-1}}$) simulated by PV_HORST in 1998, 2 years later than estimated by HORST_NH. Overall, the PVN model reproduced the magnitude and variability of observed CO_2 fluxes and is capable of reproducing the field observations.

The observations showed that CO_2 fluxes oscillated rapidly at the Ilperveld site (Fig. 3). Whilst the site had a variable water table that was above the surface, at times, the surface-height adjusted AHN water table input data reached as low at -0.75m below the surface (Fig. 2). The model results (ILP_H) reproduced a similar pattern of variability in comparison to the

https://doi.org/10.5194/gmd-2022-143
Preprint. Discussion started: 26 July 2022

observations. In 2015 and 2016, the model captured both the increasing Spring and decreasing Autumn CO_2 fluxes. The site repeatedly oscilated, within a few days, from being a CO_2 source to a CO_2 sink. PVN did a reasonable job of reproducing this variability.

PVN reproduced the mean and trend sign of CO_2 fluxes. The PVN model simulated that the 2015-17 annually averaged CO_2 emissions were 2.79 $\mathrm{kgCO_2 m^{-2} yr^{-1}}$, in alignment with the 1995-2017 annually averaged, 2.79 $\mathrm{kgCO_2 m^{-2} yr^{-1}}$(ILP_H). As with the Horstermeer scenario, PVN estimated the Ilperveld (ILP_H) annual CO_2 emissions to be larger than PV_ILP. The Peatland-VU model (PV_ILP) estimated the 2015-17 annually averaged emissions to be 1.08 $\mathrm{kgCO_2 m^{-2} yr^{-1}}$, and the 1995-2017 annually averaged CO_2 emissions to be 1.03 $\mathrm{kgCO_2 m^{-2} yr^{-1}}$.

ILP_H estimated that the maxmimum annual CO_2 emissions were 3.80 $\mathrm{kgCO_2 m^{-2} yr^{-1}}$in 2007, compared to minimum annual emissions (2.20 $\mathrm{kgCO_2 m^{-2} yr^{-1}}$) in 2006, the previous year. This is somewhat different to what was simulated by PV_ILP, which estimated that 1998 had the maximum CO_2 emissions, 1.70 $\mathrm{kgCO_2 m^{-2} yr^{-1}}$, compared to minimum emissions, 0.55 $\mathrm{kgCO_2 m^{-2} yr^{-1}}$, in 1995. The model overestimated the magnitude and variability of CO_2 fluxes variability of the fluctuating CO_2 fluxes but reproduced the same pattern of CO_2 flux variability.

3.2 Methane fluxes reproduced at both sites

The model (HORST_NH) reproduced the seasonal variability of CH_4 fluxes at the Horstermeer site (Fig. 4). The box plots showed that the model overrepresents the magnitude of peak, mean, and minimum CH_4 fluxes whilst reproducing the variability of the observational data. The PVN (HORST_NH) simulated that the 2015-17 annually averaged CH_4 emissions at the Horstermeer were 73.57 $\mathrm{gCH_4 m^{-2} hr^{-1}}$. This estimate is double the estimate of Peatland-VU, 39.17 $\mathrm{gCH_4 m^{-2} hr^{-1}}$. HORST_NH estimated the 1995-2017 annually averaged CH_4 emissions were 63.82 $\mathrm{gCH_4 m^{-2} hr^{-1}}$, about 2/3rds of the estimate made by PV_HORST, 36.99 $\mathrm{gCH_4 m^{-2} hr^{-1}}$. HORST_NH estimated that the maximum annual CH_4 emissions occurred in 2014 (84.76 $\mathrm{gCH_4 m^{-2} hr^{-1}}$), and PV_HORST estimated that they occurred in the neighbouring year, 2015 (43.65 $\mathrm{gCH_4 m^{-2} hr^{-1}}$). HORST_NH estimated that the minimum annual emissions (45.92 $\mathrm{gCH_4 m^{-2} hr^{-1}}$) occurred in 1998 and PV_HORST estimated 29.52 $\mathrm{gCH_4 m^{-2} hr^{-1}}$in 2000, 2 years later. These minimums and maximums show that, at the Horstermeer site, the 2 models responded similarly to the climatic changes during the 33 year simulation, with the maximum emissions occurring in neighbouring years and the minimum annual emissions occurring within 2 years of each other. The PVN model (HORST_NH) showed a robust agreement (R^2 = 0.61) with the observations but can overestimate the magnitude of observed CH_4 fluxes (Fig. 4).

PVN (ILP_H) reproduced the CH_4 fluxes at the Ilperveld site very well and showed a good correlation with the observations (R^2 = 0.81, Fig. 4). The model showed an increase of CH_4 fluxes during the 2015 summer (Fig. 4). Whilst, the observations did not show an increase in CH_4 fluxes at this time, this may be due to gaps in the measurements. The new PVN model (ILP_H) estimated the 2015-17, and 1995-2017 annually averaged CH_4 emissions were 4.32 $\mathrm{gCH_4 m^{-2} hr^{-1}}$and 4.02 $\mathrm{gCH_4 m^{-2} hr^{-1}}$, respectively.

The results of ILP_H estimated the 2015-17 and 1995-2017 CH_4 emissions to be approximately double the estimate made by Peatland-VU (PV_ILP). The Peatland-VU (PV_ILP) model estimated the 2015-17 and 1995-2017 annually averaged emissions

https://doi.org/10.5194/gmd-2022-143
Preprint. Discussion started: 26 July 2022

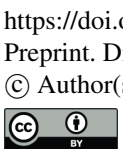

Geoscientific Model Development Discussions

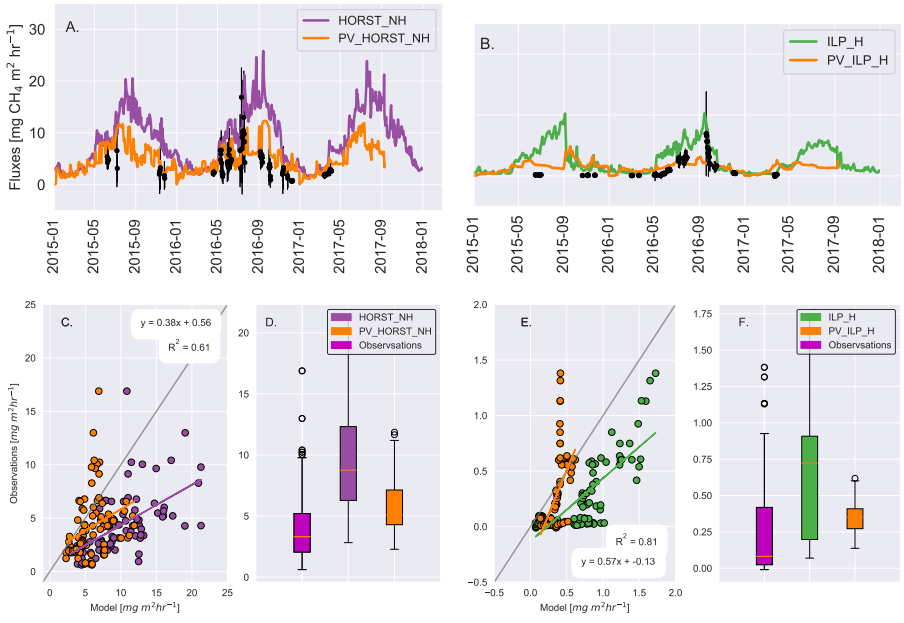

Figure 4. Simulated and observed methane fluxes at the Horstermeer (left) and Ilperveld (right). The black dots are in situ flux chamber observational measurements in panels A & B. The 1:1 line is plotted in grey. The line of the linear regression and the R^2 correlation values are provided for comparison between PVN (HORST_NH & ILP_H) and the observations. Note the differing x and y axes.

to be 2.23 $\mathrm{gCH_4m^{-2}hr^{-1}}$and 1.93 $\mathrm{gCH_4m^{-2}hr^{-1}}$, respectively. ILP_H simulated that the maximum annual CH_4 emissions occurred in 2016 (6.13 $\mathrm{gCH_4m^{-2}hr^{-1}}$) compared to minimum annual CH_4 emissions (1.51 $\mathrm{gCH_4m^{-2}hr^{-1}}$) in 1998. ILP_H estimated the maximum annual CH_4 emissions to have occured later than by PV_ILP (in 2012, 3.30 $\mathrm{gCH_4m^{-2}hr^{-1}}$). ILP_H also estimated that the minimum annual emissions occured 3 years later than PV_ILP (0.89 $\mathrm{gCH_4m^{-2}hr^{-1}}$in 1995). This shows that PVN responds to environmental conditions differently compared to Peatland-VU. At the Ilperveld site, the model reliably reproduced the trend and magnitude of observed CH_4 fluxes with an R^2 value of 0.81.

3.3 The model reproduced daily CO_2 (NEE) and CH_4 fluxes

These observations indicate that both sites are net sources of CH_4 and CO_2. These observations also show that Horstermeer produces larger peak CH_4 and CO_2 fluxes than the Ilperveld site. PVN estimated that the 2015-2017 annually averaged net GHG budgets were 3.15 (2.89) and 7.88 (3.57) $\mathrm{kgCO_{2e}m^{-2}yr^{-1}}$at Ilperveld and Horstermeer, respectively (Table 3). This is larger than estimates made by Peatland-VU; 1.27 (1.14) and 6.01 (3.72) $\mathrm{kgCO_{2e}m^{-2}yr^{-1}}$, respectively. These comparisons have shown that PVN overestimated CO_2 fluxes at the Ilperveld but did a good job reproducing the CO_2 fluxes at the Horstermeer site. PVN did a good job reproducing the magnitude and behaviour of CH_4 fluxes but overestimated the mean CH_4 fluxes. There appears to be an overall increase in the model's variability, as large CO_2 and CH_4 fluxes are overestimated, compared to earlier model versions.

https://doi.org/10.5194/gmd-2022-143
Preprint. Discussion started: 26 July 2022


Geoscientific Model Development Discussions

3.4 Plant composition is consistent at abandonment and re-establishment sites

Whilst both both sites are degraded peatlands previously used for agricultural grazing, plant composition differs between the 2 sites (Fig. 5). The Horstermeer is an unmanaged plot of land (restoration by 'abandonment'), dominated by tall grasses, sedges, *Typha* and short grasses. No mowing occurs and the HORST_NH scenario replicates the current situation. The Ilperveld is dominated by short and tall grasses, with some brown mosses, and few *Sphagnum* mosses (Fig. 5, right panel); mown twice a year and the ILP_H scenario represents the current situation.

At the Ilperveld, simulated PFT composition was compared against observational data over the years 2016 and 2017 (Fig. 5). Whereas, at the Horstermer, the simulated PFT composition was compared against observational data for the years 2006, 2016, 2017. Here we discuss both the fractional LB per square meter and fraction of LI with the observed aerial plant CF (Fig. 7). Although LB, LI, and aerial CF are not the same, we expected these variables to be insightful into the PFT composition. Plant composition observations were made at the location of the chamber measurements and were not representative of the entire site's plant community composition.

In 2006, the Hostermeer measurement location composed of short grasses (40%), reeds (50%), and tall grasses (10%) (Fig. 5). A decade later, the site had developed into tall grasses (40%), reeds (40%), short grasses (10%), and *Typha* (10%). These proportions remained consistent in Sep 2017, and October 2018. The model (HORST_NH) showed that the Horstermeer measurement site was covered by approximately 60% tall grasses, 30% sedges, and $\pm$5% *Typha* (Fig. 7). These simulated PFT proportionalities were reflected in NPP (Fig. S2), LAI (Fig. S5), PFT height (Fig. S6), litter (Fig. S8), LB (Fig. S9), and (Fig. S3). Generally, the model underestimates the amount of short grasses present. The model did a good job reproducing the proportion of sedges, *Typha* and tall grasses.

In October 2017 the Ilperveld contained *Sphagnum* moss (15%), non-*Sphagnum* moss (10%), short grass (50%), and tall grasses (25%). In November 2017, the vegetation had changed somewhat, possibly impacted by the 2017 European heatwave (García-Herrera et al., 2019), and was composed of brown mosses (10%), short grasses (80%), and tall grasses (10%). The model (ILP_H) did a good job simulating short grasses, followed by tall grasses, as the dominant plant types. The model underestimated the proportion of brown mosses, overestimated the amount of short grasses, and underestimated the proportion of tall grasses. The simulated LB of brown mosses was proportionally low, some growth was simulated by the model (ILP_H in Fig. S7). The *Omhoog met het Veen* (Raising the Peat) project delivered onsite managements attempts to initiate *Sphagnum* growth by hand dispersing living fragments of *Sphagnum* spp. from a nearby donor site between 2013 and 2015 (Geurts and Fritz, 2018). For this reason, the model does not reproduce the appearance of *Sphagnum* and brown mosses in 2017.

https://doi.org/10.5194/gmd-2022-143
Preprint. Discussion started: 26 July 2022

Geoscientific Model Development Discussions

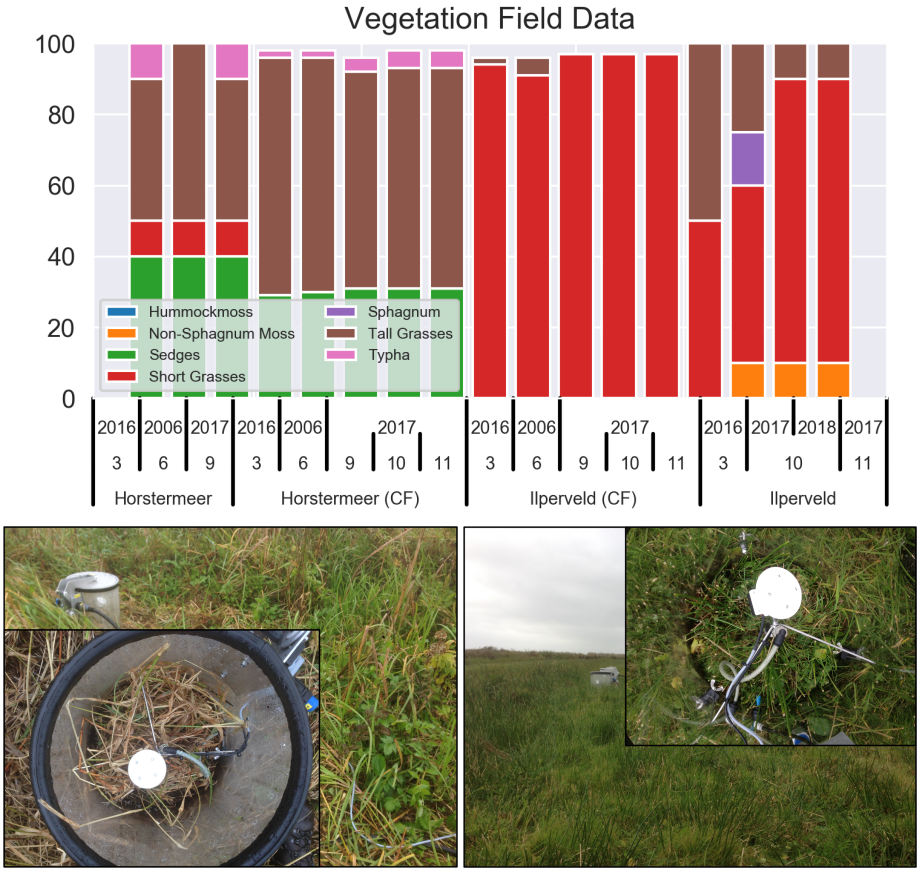

Figure 5. Simulated cover fractions (CF) and observed fractional areal vegetation types at Horstermeer (left) and Ilperveld (right). The lower panel shows the vegetation at the chamber location and the lower panel insert shows examples of the vegetation inside the chambers.

3.5 GHG emissions were large after abandonment, small after re-establishment

Here, we describe the annual net GHG emissions of multi-decadal current situation scenarios (HORST_NH & ILP_H) for the recent observational period, 2015-2017 and the period of the complete simulation, 1995-2017. To understand the impact of simulating vegetation dynamics, we compare the model results of PVN against the model results of Peatland-VU.

The model estimated that the 2015-2017 annually averaged net GHG budgets were 3.15 (2.89) and 7.88 (3.57) $\mathrm{kgCO_{2e}m^{-2}yr^{-1}}$at Ilperveld and Horstermeer, respectively (Table 3). This is larger than estimated made by Peatland-VU; 1.27 (1.14) and 6.01 (3.72) $\mathrm{kgCO_{2e}m^{-2}yr^{-1}}$, respectively. Annually averaged PVN estimates for the period 1995-2017, are larger than those estimated by the Peatland-VU model, 1.19 (1.08) $\mathrm{kgCO_{2e}m^{-2}yr^{-1}}$for the Ilperveld (PV_ILP), and 5.90 (3.73) $\mathrm{kgCO_{2e}m^{-2}yr^{-1}}$for the Horstermeer (PV_HORST) (3). PVN consistently estimated the annual net GHG budget to be larger than that estimated by the Peatland-VU model.

https://doi.org/10.5194/gmd-2022-143
Preprint. Discussion started: 26 July 2022

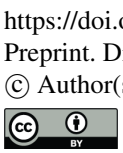

Geoscientific Model Development Discussions
Open Access
EGU

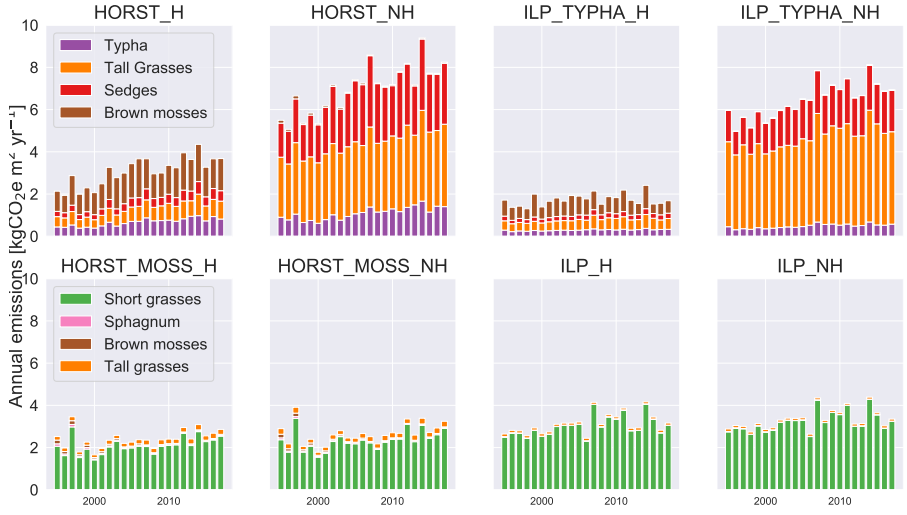

Figure 6. Simulated annual average net GHG emissions at Horstermeer and Ilperveld calculated using a 20 year Global Warming Potential. Scenarios using MOSS PFTs are in the lower panel, and scenarios using TYPHA PFTs are in the upper panel. The 1st and 3rd columns are scenarios with harvest events. The 2nd and 4th columns show scenarios without harvest events.

The Ilperveld site increased annual net GHG emissions by 0.35 (0.31) $\mathrm{kgCO_{2e}m^{-2}decade^{-1}}$ (0.03 (0.03) $\mathrm{kgCO_{2e}m^{-2}yr^{-1}}$), between 1995 and 2017. The Horstermeer site increased annual net GHG emissions by 1.38 (0.60) $\mathrm{kgCO_{2e}m^{-2}decade^{-1}}$ (0.14 (0.06) $\mathrm{kgCO_{2e}m^{-2}yr^{-1}}$), over the same period. Thereby, the annual net GHG budget at the Horstermeer was estimated to increase at a greater rate (x4) than at the Ilperveld. Carbon dioxide emissions increased by 0.029 and 0.026 $\mathrm{kgCO_{2e}m^{-2}yr^{-1}}$at the Ilperveld and Horstermeer sites, respectively, compared to CH_4 emissions, which were 6.3 $\mathrm{x10^{-5}}$ and 1.3 $\mathrm{x10^{-3}}$ $\mathrm{kgCO_{2e}m^{-2}yr^{-1}}$at the Ilperveld and Horstermeer sites, respectively. Whilst, the model results indicated that the increasing trend of GHG emissions stemmed from both increasing CO_2 and CH_4 emissions, CO_2 emissions increased at a greater rate than CH_4 emissions at both sites, and was the primary GHG contributing to increasing emissions.

The 1995-2017 annually averaged net GHG budget at the Horstermeer site (6.30 (3.28) $\mathrm{kgCO_{2e}m^{-2}yr^{-1}}$) was approximately double than the Ilperveld site(3.13 (2.89) $\mathrm{kgCO_{2e}m^{-2}yr^{-1}}$). The maximum net GHG budget at Horstermeer was 9.38 (4.41) $\mathrm{kgCO_{2e}m^{-2}yr^{-1}}$, more than double than the maximum estimated for the Ilperveld site, 4.16 (3.90) $\mathrm{kgCO_{2e}m^{-2}yr^{-1}}$2014 (2007). The minimum annual net GHG budget at the Horstermeer was 5.05 (2.30) in 1996 (1996) $\mathrm{kgCO_{2e}m^{-2}yr^{-1}}$, again more than double the minimum budget estimated for the Ilperveld, 2.44 (2.27) $\mathrm{kgCO_{2e}m^{-2}yr^{-1}}$in 2006 (2006). Throughout current situation scenarios, HORST_NH was dominated by tall grasses, sedges, and *Typha* PFTs. The current situation ILP_H scenario was dominated by short grasses with a small amount of tall grasses (Fig. 7).

https://doi.org/10.5194/gmd-2022-143
Preprint. Discussion started: 26 July 2022

Geoscientific Model Development Discussions

Table 3. Annual average CO_2, CH_4, and GHG emissions. All values are expressed as CO_2 equivalents ($kgCO_{2e}m^{-2}yr^{-1}$) and calculated using 20 (100) year GWP for CH_4 and GHG values (Eq. (20)).

Simulation Name	2015-17 GHG	1995-2017 GHG	2015-17 CO_2	1995-17 CO_2	2015-17 CH_4	1995-17 CH_4
HORST_NH	7.01 (3.60)	6.30 (3.28)	2.15	2.00	4.86 (1.45)	4.30 (1.29)
PV_HORST_NH	6.01 (3.72)	5.90 (3.73)	2.74	2.81	3.27 (0.98)	3.09 (0.92)
HORST_H	2.41 (0.96)	2.26 (0.90)	0.34	0.33	2.08 (0.62)	1.93 (0.58)
HORST_MOSS_H	2.26 (0.73)	2.12 (0.69)	0.09	0.08	2.17 (0.65)	2.04 (0.61)
HORST_MOSS_NH	2.90 (0.85)	2.60 (0.76)	-0.02	-0.02	2.91 (0.87)	2.62 (0.78)
ILP_H	3.16 (2.90)	3.13 (2.89)	2.79	2.79	0.37 (0.11)	0.34 (0.10)
PV_ILP_H	1.27 (1.14)	1.19 (1.08)	1.09	1.03	0.19 (0.06)	0.16 (0.05)
ILP_NH	3.36 (3.06)	3.34 (3.06)	2.94	2.94	0.43 (0.13)	0.39 (0.12)
ILP_TYPHA_H	1.59 (1.38)	1.73 (1.55)	1.28	1.47	0.31 (0.09)	0.03 (0.08)
ILP_TYPHA_NH	6.99 (6.42)	6.43 (6.02)	6.18	5.85	0.81 (0.24)	0.58 (0.17)

3.6 Rewetting scenarios impact GHG emissions

To investigate the influence of vegetation on GHG emissions, we compare the model results of 2 different restoration scenarios, re-establishment and abandonment. To replicate re-establishment efforts at the Horstermeer site, the site was simulated with MOSS PFTs, with and without harvests (HORST_MOSS_H & HORST_MOSS_NH) and to replicate restoration by abandonment at the Ilperveld site, the site was simuated with TYPHA PFTs, with and without harvests (ILP_TYPHA_H & ILP_TYPHA_NH). An overview of the model scenarios is provided in Table 2. The relative contributions of each PFT towards annual net GHG emissions are plotted in Fig. 6. Figure 8 compares the net GHG emissions of model scenarios using the TYPHA and MOSS PFT compositions. An overview of the statistics of the model results is provided in Table 3.

The MOSS PFT scenarios (HORST_MOSS_NH, HORST_MOSS_H) reduced the annual CO_2 and CH_4 fluxes at the Horstermeer site, compared to the current situation (HORST_NH). The 2015-17 annually averaged net GHG emissions of HORST_MOSS_NH was approximately half the emissions (2.9 (0.9) $kgCO_{2e}m^{-2}yr^{-1}$) of the current situation scenario (HORST_NH, 7.0 (3.6) $kgCO_{2e}m^{-2}yr^{-1}$). Short grasses were the dominant PFT (>80%) in HORST_MOSS_NH and HORST_MOSS_H, a similar result to what was found in MOSS Ilperveld scenarios, ILP_H and ILP_NH. When harvests were included in the Horstermeer MOSS scenario (HORST_MOSS_H), there was only a minor reduction in annual GHG emissions, to 2.3 (0.7) $kgCO_{2e}m^{-2}yr^{-1}$. These model results showed that the presence of the MOSS PFTs have the potential to reduce GHG emissions (Fig. 6).

The TYPHA PFT composition (*with harvests*, ILP_TYPHA_H) reduced the GHG emissions at the Ilperveld site to 1.6 (1.4) $kgCO_{2e}m^{-2}yr^{-1}$(2015-17 annual average). The TYPHA PFT scenarios (*with harvests*, ILP_TYPHA_H) reduced the annual CO_2 and CH_4 fluxes at the Ilperveld site, compared to the current situation (ILP_H). The TYPHA PFT scenario, *without harvests*, led to increased GHG emissions, 7.0 $kgCO_{2e}m^{-2}yr^{-1}$. This results show that the TYPHA scenario at the

https://doi.org/10.5194/gmd-2022-143
Preprint. Discussion started: 26 July 2022

Geoscientific Model Development Discussions
Open Access
EGU

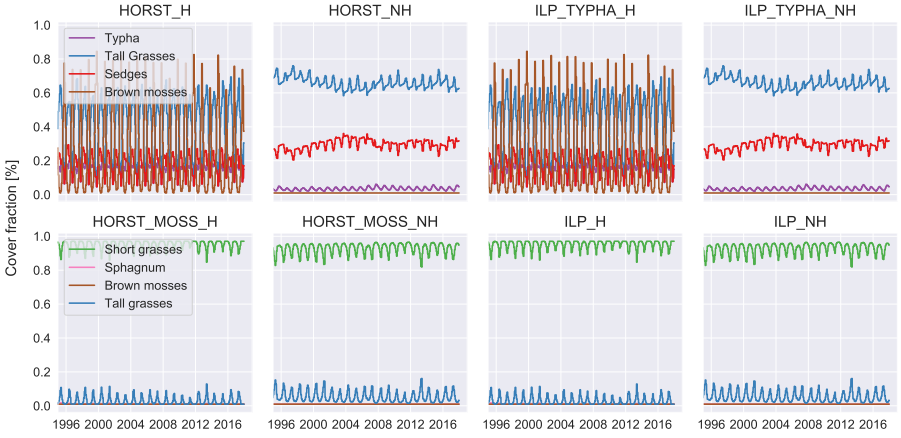

Figure 7. Monthly average cover fractions. Scenarios using MOSS PFTs are in the lower panel, and scenarios using TYPHA PFTs are in the upper panel. The 1st and 3rd columns are scenarios with harvest events. The 2nd and 4th columns show scenarios without harvest events.

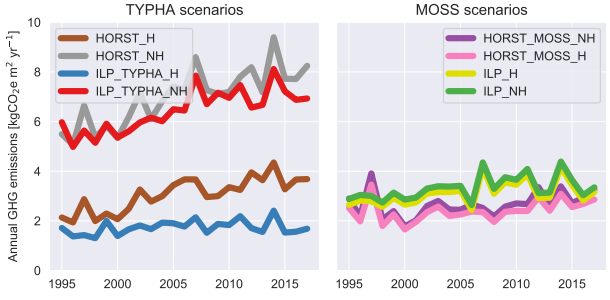

Figure 8. Simulated annual average net GHG budgets for scenarios using the TYPHA PFTs (left) and MOSS PFTs (right). The GHG budget was calculated using a 20 year GWP.

Ilperveld had the potential to both increase or decrease annual net GHG emissions, depending on whether harvests occured. The dominant PFTs in the ILP_TYPHA_H scenario were tall grasses and brown mosses, with a small presence of sedges and Typha. This composition of PFTs somewhat differs to what was dominant in the HORST_H scenario (brown mosses, tall grasses, *Typha*, sedges). Despite having the same climatic input, the different soil, water table and model input parameters develop different PFT proportionality. This finding suggests that abandonment restoration efforts can lead to different PFT proportionality depending on site conditions.

3.6.1 Rewetting method impacts GHG emissions

The largest annual average GHG emissions were produced by the two scenarios with TYPHA PFTs and *without* harvests ('_NH'), ILP_TYPHA_NH and HORST_NH, i.e. the abandonment rewetting pathway. The GHG emissions for ILP_TYPHA_NH

https://doi.org/10.5194/gmd-2022-143
Preprint. Discussion started: 26 July 2022


Geoscientific Model Development Discussions

and HORST_NH were 6.4 & 6.3 $\mathrm{kgCO_{2e}m^{-2}yr^{-1}}$, respectively. The smallest annually averaged GHG emissions were produced a scenario with TYPHA PFTs but including harvests, ILP_TYPHA_H (1.73 $\mathrm{kgCO_{2e}m^{-2}yr^{-1}}$).

We found that the GHG emissions were reduced for ILP_TYPHA_H and for HORST_MOSS_NH compared to the current situation scenarios, ILP_H and HORST_NH, respectively. Here we assess the differences in CO_2 and CH_4 fluxes between ILP_H & ILP_TYPHA_H and HORST_NH & HORRST_MOSS_NH. Carbon dioxide and CH_4 fluxes reduced for HORST_MOSS_NH, compared to HORST_NH. This was an expected result because we expected the MOSS PFTs to lead to a similar result to what was found for ILP_H. Carbon dioxide and CH_4 fluxes reduuced for ILP_TYPHA_H compared to ILP_H. This was an unexpected result because we expected the TYPHA scenario to result in sedges and Typha PFTs sharing the majority of PFT proporionality and lead to increaed CO_2 and CH_4 emissions. However, we found the plant dynamics led to brown mosses and tall grasses sharing the majority of PFT proportionality, leading to low CO_2 and CH_4 emissions.

3.6.2 Site properties impact CO_2 and CH_4 emissions

Here, we look at the drivers of annual CO_2 (Fig. 9) and CH_4 (Fig. 10) emissions. ILP_TYPHA_NH produced the largest annually averaged CO_2 emissions (5.9 $\mathrm{kgCO_2m^{-2}yr^{-1}}$) compared to other scenarios. All other scenarios produced annually averaged CO_2 emissions < 3 $\mathrm{kgCO_2m^{-2}yr^{-1}}$. The smallest annual average CO_2 emissions were produced by HORST_MOSS_NH (-0.02 $\mathrm{kgCO_2m^{-2}yr^{-1}}$). The annual CO_2 emissions of HORST_MOSS_H were also small (< 1 $\mathrm{kgCO_2m^{-2}yr^{-1}}$). Ilperveld tended to produced larger annual CO_2 emissions than the Horstermeer, but this was not true for all cases.

The scenario with the largest annually averaged CH_4 emissions was HORST_NH (4.3 $\mathrm{kgCO_{2e}m^{-2}yr^{-1}}$). This was followed by HORST_MOSS_NH (2.62 $\mathrm{kgCO_{2e}m^{-2}yr^{-1}}$), HORST_MOSS_H (2.04 $\mathrm{kgCO_{2e}m^{-2}yr^{-1}}$), and HORST_H (1.93 $\mathrm{kgCO_{2e}m^{-2}yr^{-1}}$). The remainder of scenarios produced annually averaged CH_4 emissions < 1 $\mathrm{kgCO_{2e}m^{-2}yr^{-1}}$. Horstermeer consistently produced CH_4 emissions that were larger than those simulated for the Ilperveld.

3.6.3 Harvests impact PFT composition for TYPHA scenarios

Here we investigate the role of harvests on plant dynamics. Differences between TYPHA scenarios and small between MOSS scenarios (Fig. 7). To assess the impact of harvest at the Horstermeer, we compared simulations HORST_H (with harvests) and HORST_NH (without harvests). large differences were found between scenarios, HORST_H and HORST_NH. Small, or no, differences were observed between HORST_MOSS_NH and HORST_MOSS_H. PFT composition was similar, as were CO2, CH4, and GHG emissions.

We took a close look at PFT dynamics using scenario HORST_H, short grasses increased due to reduced shading and increased light availability (Fig. 7). Following harvest events, short grasses intercepted ±60% of incoming light compared to ±5% before the harvest event. In the period between 2 harvests, tall grasses increased CF to 80%, and sedges increased CF from 5% to 25%, *Typha* increased by 5-10%. Harvest events reduced the height advantage of tall plants to intercept light. Fig. S6 shows the height change per PFT and Fig. S5 shows the impact on LAI. The LAI of brown mosses reached 1.5 $\mathrm{m^2m^{-2}}$, in scenarios ILP_TYPHA_H and HORST_H, but remained less than 0.5 $\mathrm{m^2m^{-2}}$ in ILP_TYPHA_NH and HORST_NH sce-

https://doi.org/10.5194/gmd-2022-143
Preprint. Discussion started: 26 July 2022

Geoscientific Model Development Discussions
Open Access
EGU

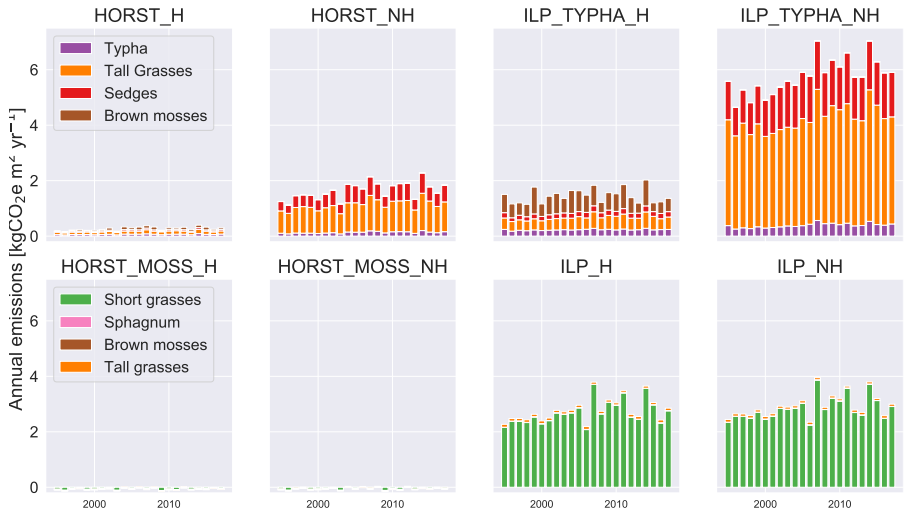

Figure 9. Simulated annual average CO_2 emissions, calculated using a 20 year GWP. Scenarios using MOSS PFTs are in the lower panel, and scenarios using TYPHA PFTs are in the upper panel. The 1st and 3rd columns are scenarios with harvest events. The 2nd and 4th columns show scenarios without harvest events.

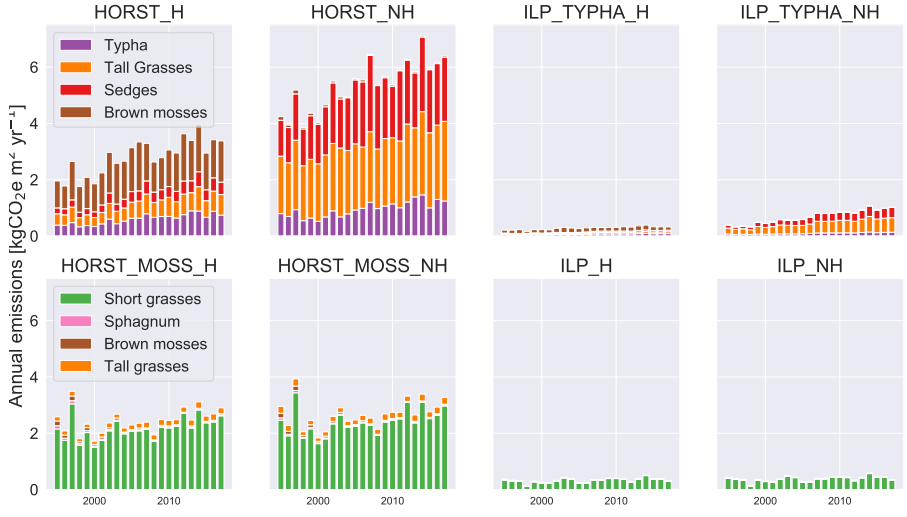

Figure 10. Simulated annual average CH_4 emissions, calculated using a 20 year Global Warming Potential. Scenarios using MOSS PFTs are in the lower panel, and scenarios using TYPHA PFTs are in the upper panel. The 1st and 3rd columns are scenarios with harvest events. The 2nd and 4th columns show scenarios without harvest events.

narios. Without harvest events, tall plants maintained a height advantage over short plants, intercepting approximately 80% of incoming light.

https://doi.org/10.5194/gmd-2022-143
Preprint. Discussion started: 26 July 2022

To assess the impact of harvests at the Ilperveld, we compared simulations ILP_H (with harvsts) against ILP_NH (without harvests) and ILP_TYPHA_NH against ILP_TYPHA_H. Little or no difference was seen when comparing PFT proportionality in scenario ILP_NH compared to ILP_H. PFT LI fractions at the Ilperveld were similar for Ilperveld MOSS simulations with and without harvest. Large differences were seen in the plant compositions of ILP_TYPHA_NH against ILP_TYPHA_H. ILP_TYPHA_NH was doinated by tall grasses, and sedges with some Typha. ILP_TYPHA_H was dominated by brown mosses, tall grasses with presence of *Typha* and sedges. Differences in CO2 and CH4 emissions were also large.

These results showed harvests acted as a mechanism that increased the competitiveness of short plants against tall plants. Harvests reduced the LB of tall PFTs, enabling short PFTs greater access to resources, which led to an overall reduction the net GHG emissions, and particularly the annual CO_2 emissions. These results indicate harvests play a large role on plant dynamics for the TYPHA scenario but not the MOSS scenario.

3.6.4 Harvests scenarios reduced GHG emissions for TYPHA scenarios

Beyond differences in the PFT CF, LB and LI, CO_2 and CH_4 emissions varied due to harvest (Fig. 7). Comparing simulations with and without harvests (Table 3 & Fig. 8), showed that the annual GHG emissions were smaller for scenarios *including* harvests. Differences in the GHG emissions between HORST_MOSS_NH & HORST_MOSS_H and ILP_H and ILP_NH were small. However, differences in the GHG emissions between HORST_NH & HORST_H and ILP_TYPHA_H and ILP_TYPHA_NH were large. At the Horstermeer, the 2015-2017 annually averaged GHG emissions were estimated to be smaller with the occurence of harvests 2.08 (0.87) $\mathrm{kgCO_{2e}m^{-2}yr^{-1}}$(HORST_H), compared to the current situation scenario, HORST_NH. It is likely that harvests impacted GHG emissions by limiting tall plants that are very productive and often function as large gas conduits, and allowing light access for short plants. At the Ilperveld, the 2015-2017 annually averaged GHG emissions were sightly larger without harvests (ILP_NH), 3.35 (3.06) $\mathrm{kgCO_{2e}m^{-2}yr^{-1}}$, compared to 3.15 (2.88) $\mathrm{kgCO_{2e}m^{-2}yr^{-1}}$, with harvests (ILP_H). Aligned with the fingings that harvests played a larger role on plant dynamics in TYPHA scenarios, compared to MOSS scenarios, the results showed that the impact of harvests on GHG emissions wass greater for TYPHA scenarios than for MOSS scenarios (Fig. 8).

4 Discussion

Using PVN, a dynamic vegetation-emissions model, we reproduced observed greenhouse gas fluxes on daily and seasonal scales and plant community composition at 2 field sites. We estimated the 2015-2017 annually averaged net GHG budgets to be 3.2 and 7.8 kg $\mathrm{kgCO_{2e}m^{-2}yr^{-1}}$, at the Ilperveld and Horstermeer sites respectively. These estimates were compared to unpublished chamber observations and an earlier version of the model, previously used to make estimates of peatland net GHG budgets. We found that the of harvest events mimics landscape scale competition between PFTs. We assessed the impact of hypothetical plant communities by swapping the plant compositions of the 2 sites. We found that the re-establishment scenario (MOSS PFTs & harvests) reduced annual net GHG emissions by more than 50% at the Horstermeer site and that abandonment scenario (TYPHA scenario without harvests) increased GHG emissions by 30% at Ilperveld site. These results indicate that

https://doi.org/10.5194/gmd-2022-143
Preprint. Discussion started: 26 July 2022

Geoscientific Model Development Discussions

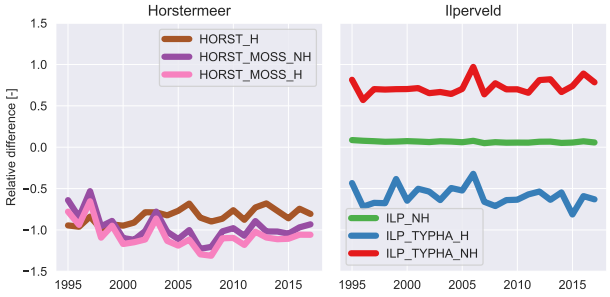

Figure 11. Relative simulation differences of GHG emissions for the Horstermeer (left) and Ilperveld (right) sites, as the natural logarithm of the model scenario result over the current situation scenarios, HORST_NH (left) and ILP_H (right), respectively.

plant community re-establishment efforts and the occurrence of harvests play an important role on restored peatland GHG emissions.

4.1 Plant communities' impact GHG emissions

The PVN model results indicated that sedges and tall grasses have the potential to enhance annual CO_2, CH_4, and net GHG emissions. Mowing (harvests) have the potential to reduce CO_2, CH_4, and GHG emissions in sites where tall plants (e.g. sedges, tall grasses, Typha) are present. We found that short lawn grasses were competitive against other PFTs. We used the natural logarithm to compare the relative difference between the multiple model scenarios and HORST_NH & ILP_H, the current situation scenarios (Fig. 11). We found less variation in net GHG emissions between scenarios including MOSS PFTs than between scenarios including TYPHA PFTs (Fig. 8), indicating that the presence of MOSS PFTs have the potential to reduce GHG emissions. These model results indicate that TYPHA PFTs would likely increase the GHG budget at restored peatland sites and that mowing (harvests) have the potential to reduce GHG emissions.

We found it promising that model was sensitive to root exudation, and that the exudation parameter (ExudateFactor) played an important role determining the PFT CH_4 flux. Root exudation plays an important role in the rhizosphere by promoting methanogensis and soil carbon loss through CH_4 (Philippot et al., 2009). Exudates develop at a prescribed rate per PFT which is dependent on root and shoot growth (dependent on photosynthesis, ideal and tolerated water table limits). With higher NPP, plant photosynthates are allocated to the rhizosphere where the root exudates provide carbon for soil microbial communities to metabolise into CH_4 (Paudel et al., 2016; Philippot et al., 2009). Root traits play an important role in species competition (Iversen et al., 2015) and PFT observational data, such as exudation rates, root mass and shoot mass, would help improve future versions of the model.

These results are aligned to previous field studies which have shown relationships between individual species, CH_4 emissions, and carbon turnover (*Carex*, *Phragmitis*, and *Typha* (Günther et al., 2014); *Eriophorum vaginatum*, *Carex rostrata* and *Juncus effusus* (Ström et al., 2005)). However, these studies are short term (<5 year periods) and focus on monocultures, or single species, with no or few studies investigating the role of ecosystem composition.

https://doi.org/10.5194/gmd-2022-143
Preprint. Discussion started: 26 July 2022


Geoscientific Model Development Discussions

570 To maintain a sense of realism in this study, we swapped the plant composition of both sites rather than composing fictitious community compositions. An assessment of these 3 scenarios showed 3 potential pathways to reduce annual net GHG emissions at the Horstermeer (Fig. 11). At the Ilperved, these scenarios showed that an abandoment restoration pathway would have resulted in larger GHG emissions than the followed re-establishment pathway. Further studies might investigate the impact of decreasing or increasing diversity of plant types to quantify the impact of changing biodiversity on peatland GHG emissions.
575 Another use of the model may be to assess the impacts of extreme climate events (such as extreme rainfall, drought, heatwaves) on plant competition and associated peatland GHG fluxes.

4.2 Harvests impacts plant competition and GHG emissions

The model results indicated that harvest had the potential to play a large role, acting as plant competition mechanism, impacting seasonal CO_2 & CH_4 fluxes, and annual GHG emissions. At the Horstermeer, biannual harvests reduced the 2015-2017 annu-
580 ally averaged GHG emissions, by ¾, from 7.9 (HORST_NH) to 2.1 $\mathrm{kgCO_{2e}m^{-2}yr^{-1}}$(HORT_H). At the Ilperveld, harvests marginally reduced the annually averaged net GHG emissions (Fig. 8). Therefore, harvests may have a large influence on plant dynamics and composition but this is dependent on the PFTs included in the scenario (i.e. prescribed PFTs).

Whilst many studies have investigated the impact of harvest on specific species and monocultures), few or no studies have investigated the impact of harvest on entire peatland ecosystems. The inclusion of harvest has proven necessary to to reproduce
585 the seasonal variability of fluxes in grasslands and crops, where crop harvests occur (Van den Hoof et al., 2011). The harvest method implemented in PVN was similar to the instantaneous harvest method featured in other dynamic vegetation models (such as JULES (Littleton et al., 2020), where the plant is reduced to a certain set height and living biomass and LAI are subsequently adjusted accordingly. JULES assumes 100% of lost biomass is harvested whilst killing off a proportion of belowground biomass that is converted to litter. The PVN model assumes 20% of harvested biomass is lost to litter and does not account for
590 root death. Living biomass decreased by the proportional biomass lost, assuming the plant's biomass is uniformly distributed with height, and LAI is recalculated. Root mass observational measurements over time as well as observational data on the impact of harvests on plant health (or productivity) would be helpful to further improve model representations of harvests.

4.3 Horstermeer and Ilperveld are small net C sources

The GHG emissions of the sites assessed in the present study have similar, but larger emissions compared to other restored
595 peatlands. A comparison of drained and restored peatlands in the Sacramento-San Joaquin Delta of California, found that drained sites were net C and GHG sources, releasing up to 341 $\mathrm{gCm^{-2}yr^{-1}}$in the form of CO_2 (1 $\mathrm{kgCO_2m^{-2}yr^{-1}}$) and 11.4 $\mathrm{gCm^{-2}yr^{-1}}$in the form of CH_4 (15 $\mathrm{gCH_4m^{-2}hr^{-1}}$or 42 $\mathrm{gCO_{2e}m^{-2}yr^{-1}}$) (Knox et al., 2015). Conversely, restored wetlands were net sinks of atmospheric CO_2, sequestering up to 397 $\mathrm{gCm^{-2}yr^{-1}}$(2 $\mathrm{kgCO_2m^{-2}yr^{-1}}$) but were large sources of CH_4, with emissions ranging from 39 to 53 $\mathrm{gCm^{-2}yr^{-1}}$(0.2 $\mathrm{kgCO_{2e}m^{-2}yr^{-1}}$) (Knox et al., 2015). This equates to an annual net
600 GHG balance of 43.3 $\mathrm{kgCO_{2e}m^{-2}yr^{-1}}$for drained sites, and -1.65 $\mathrm{kgCO_{2e}m^{-2}yr^{-1}}$for restored sites. An explenation of the differences observed between the present study and the study of Knox et al. (2015) are likely due to differences in measurement method. Chamber measurements (used in the present study) are not representative of the site's flux average, whereas, EC tower

https://doi.org/10.5194/gmd-2022-143
Preprint. Discussion started: 26 July 2022


Geoscientific Model Development Discussions

data reports spatial averages. Beyond this, the AC chamber method is known to overestimate fluxes, whereas the EC method is known to underestimate fluxes. The GHG emissions of the sites assessed in the present study have similar, but larger emissions to other restored sites but are sources, rather than sinks, of CO_2 and CH_4 emissions.

4.4 PVN incorporates functionality of NUCOM

(refer to PFT results and maybe shorter) PVN has incorporated aspect of the NUCOM-BOG model into the Peatland-VU model. PVN includes competition between species and the impact of species on important above and belowground ecosystem processes such as C sequestration, and CH_4 processes (decomposition, production, ebullition, diffusion), CO_2 & CH_4 plant transport, decomposition, plant photosynthesis, plant respiration, and PFT competition due to water availability, (ideal & tolerated) temperature growing limits, height & subsequent shading. Root mass, density and root depth was made PFT specific in this new version of the model and thereby enabled competition in relation to the water level and soil moisture. Photosynthesis and plant respiration are calculated per PFT and the amount of available shortwave radiation available is determined by light availability due to shading, in accordance to plant height and LAI. Height growth is calculated using a height-biomass depth relationship (Huang et al., 1992). LAI was adapted from (Heijmans et al., 2008) and is a function relating LB, specific leaf area, light extension coefficient, and water availability. LAI exhibits both seasonal and long-term variability. The depth of moss growing on the surface taken from (Heijmans et al., 2008) has the potential to be incorporated into the soil layer, altering the relative height of the land surface (relative to the water table, for example) and corresponding soil layer properties (e.g. pH, DBD).

Light interception fractions were generally more sensitive than and showed larger seasonal variations compared to CF (fractional LB) (Fig. 7). It's worthwhile to note that after the spin-up period the model equilibrated to the same PFT ratios, regardless of the prescribed PFT CF. The model did a very good job reproducing seasonal variations in CFs at both sites and in response to harvest events.

Observed data focuses on aboveground processes (e.g. photosynthesis, litter, respiration, living aboveground biomass) with considerably less attention being paid to belowground processes (exudation, root and shoot biomass, microbial activity), possibly due to the invasiveness of belowground sampling. Representation of belowground processes are critical to reliably simulate peatland GHG fluxes but are accompanied by persistent uncertainties. Field campaigns targeting belowground observations will aid model representation of belowground peatland processes. Studies investigating the impact of climate change on GHG emissions in restored peatlands must focus efforts on assessing the interactions within maturing ecosystems and the impacts of various changing climate drivers on complete ecosystem functioning.

4.5 Daily variability of CO_2 and CH_4 fluxes were well represented with uncertainties

Whilst the model appears to reproduce the mean and magnitude of CO_2 fluxes, the model may not be aptly responding to environmental changes. Whilst, the CH_4 fluxes may not agree in mean, spread, and slope of linear regression, the R^2 value is high. This suggests that the CH_4 model responds well to the environmental processes but struggles to produce the same magnitude of response. Due to the chamber technique, known uncertainties exist in the observational dataset used for model validation.

https://doi.org/10.5194/gmd-2022-143
Preprint. Discussion started: 26 July 2022


Geoscientific Model Development Discussions

for example, during the night, water condenses on the inside of the chambers, which candecrease the amount of incoming light, and reduce early-morning photosynthesis. The chambers can create a small greenhouse effect, potentially increasing CH_4 production. As a consequence, CH_4 emissions may be overestimated whilst CO_2 emissions may be underestimated.

4.6 Water table input data may not be locally accurate

The NHI-AHN water table product was used in this study in an attempt to improve upon the simple water table model built in to the model, and is accompanied by uncertainties. Whilst, previous studies have emphasised the benefits of using the output of general circulation models to reproduce water table estimates longer than the observational record (Wania et al., 2009), the water table input data, at times, resulted in a considerably low water table, 0.6 – 0.7m below the surface, which may not be realistic. Further, using a prescribed water table prevents the simulation of dissolved gases in water. The product used to determine the water table was initially a x250m gridded product and adjusted to be relative to surface using a x0.5m digital surface elevation model. Ditches, polders, and polder boundaries, impact the surface water table, occur at distances less than 250m, which was either not adequately addressed by AHN or the low water table levels are a result of model uncertaintities in NHI.

4.7 The Horstermeer site is highly heterogenous

We compare the findings of this study against other studies that have assessed GHG fluxes at the Horstermeer site. Unfortunately, at the time of publication there were no published studies investigating GHG fluxes at the Ilperveld. The estimates in the present study were higher than estimates for 3 peatland sites in the Netherlands (Schrier-Uijl et al., 2014), one of which was the Horstermeer. The differences in the fluxes recorded at the Horstermeer are likely due to the measurements being taken at different locations within the heterogeneous site. The present study measured fluxes in the range of 0-17 $\mathrm{mgCH_4m^{-2}hr^{-1}}$(2015-17) compared well to chamber CH_4 fluxes, in the range of 2-15 $\mathrm{mgCH_4m^{-2}hr^{-1}}$, measured from 2003 till 2008 (van Huissteden et al., 2009) at an area of the site with a varying water table. The CH_4 measurements, presented in this study between 2015 and 2017, made in a wet area at the Horstermeer were more than double the measurements measured in dry areas of the Horstermeer between 2004 and 2006, using the manual chamber technique (Hendriks et al., 2007). The different chamber measurement technique may account for the observed differences. The 2015-17 fluxes were measured at 15 minute intervals using semi-automatic chambers that operated 24 $\mathrm{hrday^{-1}}$, converted to daily and hourly averages; whereas the 2004-06 fluxes were measurements were made during daytime hours only, and converted to hourly values. CH_4 fluxes are smaller during the night (Long et al., 2010) and therefore, measurement techniques that only measure during the day are likely overestimate the daily hourly average.

We compared the PVN and Peatland-VU models against FLUXNET data at the Horstermeer site Fig. . CH_4 observations from the FLUXNET dataset are 1-2 $\mathrm{mgCH_4m^{-2}hr^{-1}}$, much lower than the 2004-06 observations of previous studies (Hendriks et al., 2007), the 2015-17 observations, and the modelled estimates. The portion of the site included in the EC tower's footprint is dependent on wind speed and direction. Fluxes in dry areas of the site are, on average, 1/3rd of fluxes in wet areas. The site is for the most part a dry peatland, except for the perimeters that border ditches. Thereby, it is likely that the CH_4 flux of the

https://doi.org/10.5194/gmd-2022-143
Preprint. Discussion started: 26 July 2022


Geoscientific Model Development Discussions

dry areas dominate the EC tower footprint. Site heterogeneity (both vegetation and relative water table height), and particularly the proportion of saturated land surface vs. unsaturated land surface may explain the differences between 2006-09 EC tower and the 2015-17 chamber observations.

4.8 Site heterogeneity is difficult to reproduce in peatland models

PEATBOG (Wu and Blodau, 2013) is the only other site specific peatland model that simulates CO_2 and CH_4 fluxes and includes competition between PFTs. Like the Peatland model, PEATBOG has a large amount of input model parameters. PEATBOG simulated the Mer Bleue Bog in Canada, a pristine (untouched) raised acidic ombrotrophic bog, over a 6 year period. The Mer Bleue Bog is a nutrient poor bog, dissimilar to the two sites assessed in this study. Peat has been accumulating at this site since 8400 calyrBP and has developed a peat depth of 6m in the centre. PEATBOG accounts for similar biogeochemical processes as the PVN model but also includes nitrogen cycling, and subsequent dissolved C (DIC, DOC), CO_2 and CH_4 run-off. PEATBOG underestimated the annual net GHG emissions (net ecosystem carbon balance), by approximately half of observed field observations. The annual Mer Bleue Bog emissions were approximately 1/50th of the Ilperveld GHG emissions. Wu and Blodau (2013) noted the sensitivity of PEATBOG to temperature, reporting that 1 °Cof temperature change was enough to initiate a model bias, swaying the model from a sink to a source. It appears that the PEATBOG represents many complex processes, some of which were beyond the scope of PVN, and does a good job reproducing daily NEE, ER, and GPP but is unable to reproduce the total annual net carbon budgets. This suggests that there was difficulty reproducing CH_4 fluxes, particularly the peak summer CH_4 fluxes, and spikes in CH_4 fluxes catalysed by a rapidly changing water table. Whilst, the simulated and observed DOC runoff values were in good agreement, dissolved CO_2 and CH_4 lost in runoff were underestimated by the model, dampening the already underestimated net GHG budget. Thereby it may have been the sensitivity of the CH_4 submodule to changes in climate (temperature, precipitation, water table), dissolved CO_2 and CH_4 that impacted the ability of the PEATBOG model to simulate the site's net C budget. Further, the complexity of calibrating a landscape scale model may contribute to the model's abilities.

4.9 PVN may produce larger than observed fluxes

PVN estimated the 1995-2017 annually averaged net GHG budget to be larger than the Peatland-VU model, at both sites. This is seen in the long-term behaviour of Peatland-VU model results where there is a CO_2 emissions (NEE), and an increasing trend in CH_4 emissions, at both sites. The belowground CH_4 pools in the Peatland-VU model increased consistently during the model simulation and therefore, an increasing quantity of CH_4 was released from the soil profile throughout the simulation, meaning that the fluxes were likely underestimated early in the simulation. The comparatively large estimates of fluxes made by PVN as compared to Peatland-VU need further study to determine which model structure changes are responsible for this. For example, the sum of PFTs may result in values above the ecosystem total. Further modelling efforts could investigate how to better constrain this. PVN prescribes different PFTs to have root and shoot mass and root depths. This means CH_4 and carbon pools are being accessed in different soil layers for each PFT. Carbon pools are divided between active and inert carbon per timestep per PFT, for each soil layer and for each OM pool. The OM pools defined by the model as a singular matrix and includes

https://doi.org/10.5194/gmd-2022-143
Preprint. Discussion started: 26 July 2022


Geoscientific Model Development Discussions
Open Access
EGU

labile, manure, peat, exudates, litter and roots, microbes, humus forms of SOM. These ecosystem variables became PVN PFT variables. Further model efforts could work to separate the matrix so that exudates, litter, roots, microbes, labile, and humus are calculated per PFT but manure and peat are calculated as ecosystem totals. CH_4 fluxes arising from decomposition of the peat SOM pool only come from the moss PFTs in the PVN model. CH_4 fluxes arising from litter, exudates came from all PFTs. CH_4 fluxes arising from roots comes from non-moss PFTs. Mosses are considered to have maximum 0.1m roots when the model is initialised. However, these roots do not grow or die throughout the model simulation. Mosses do not have an aboveground litter layer and instead their living biomass after senescence, is added directly to the belowground OM. The peat-SOM pool of moss PFTs contribute to CO_2 and CH_4 fluxes because (*Sphagnum*) mosses are the primary peat-contributing plant and this is because mosses (especially *Sphagnum*) decompose very slowly (Hobbie et al., 2000). Total decomposition is dependent on the decomposition rates of different plants which generally follow this order (rates of breakdown varying in the following order: forbs, graminoids, deciduous shrubs, evergreen shrubs (Dorrepaal et al., 2006, 2007, 2009) and the proportional litter mass which is dependent on the proportion of PFTs present as well as the microbial activity influenced by nutrient availability, soil temperature, pH etc (Bardgett et al., 2008). Plant respiration is calculated as a function of leaf respiration, photosynthesis, and light availability. Light availability, LAI, and leaf respiration were set Peatland-VU values. The PVN photosynthesis module calculates light availability based on height, LAI, and shading. Leaf respiration coefficient is prescribed per PFT and taken from the literature. We found that enabling different PFTs to contribute to, oxidise, and decompose different belowground SOM pools, impacted CO_2 and CH_4 production. The storage of CO_2 and CH_4 in multiple PFT pools, respond at different moments to environmental factors, which results in consistent fluxes over long model simulations.

4.10 The impact of climate change is evident

Climate change is likely to impact precipitation, temperature, and weather patterns, all of which are known environmental drivers of peatland GHG emissions. Few (or no) long term analyses have assessed long term changes to peatland GHG emissions in the Netherlands, and therefore it is a useful tool to discuss the potential role of climate change. Both temperature-driven changes in reaction rates and changes in C pools could drive the increase in GHG emissions; the model also allows the analysis of combined effects of C pool and temperature change, which is a subject of further analysis. Daily temperature observations show local temperatures increased by +0.1C $^{\circ}\mathrm{Cyr}^{-1}$in the very recent past, between 2010 and 2017, compared to +0.06 $^{\circ}\mathrm{Cyr}^{-1}$over the entire simulation period (1996-2017). At the Ilperveld site, model results estimated GHG emissions increased by 0.35 (0.31) $^{\circ}\mathrm{Cdecade}^{-1}$, or 0.03 (0.03) $\mathrm{kgCO_2m^{-2}yr^{-1}}$between 1995 and 2017. This rate of increase is grater than estimated for the Horstermeer. At the Horstermeer site, model results estimated GHG emissions increased by 1.4 (0.60) $^{\circ}\mathrm{Cdecade}^{-1}$between 1995 and 2017, or 0.14 (0.06) $^{\circ}\mathrm{Cyr}^{-1}$.

It is likely that peatlands across the globe will respond to differently to climate change and therefore, the net global magnitude and even the sign of feedback of peatlands responding to climate change is still unknown (Gorham, 1991; Olefeldt et al., 2013). Future projections have estimated that on average, globally, peatlands will remain similarly wet but become warmer, leading to increased soil surface temperatures, increased oxidation, microbial activity, and enhanced CH_4 release (Melton et al., 2013; Wania et al., 2009). An alternative outcome of wetter warmer environments may be peat development and carbon sequestration.

https://doi.org/10.5194/gmd-2022-143
Preprint. Discussion started: 26 July 2022


Geoscientific Model Development Discussions

The increase in net GHG emissions is largely due to increasing CH_4 emissions. Annual CO_2 emissions were stable at both sites. At these sites, precipitation was annually consistent over the simulated period, whilst temperatures increased. These model simulations indicate that processes leading to increased CH_4 emissions outweigh the potential for peat development at these two assessed sites in the Netherlands.

PVN 1.0 was developed by building upon the functionality and structure of Peatland-VU whilst incorporating vegetation dynamics from the NUCOM model. The PVN has incorporated vegetation dynamics and enhanced PV's already existing carbon cycling processes. Competition is based on water table depth, temperature, height and shading, moss depth. PVN has taken the LAI function from NUCOM and developed it to exhibit both seasonal and long-term variations. Nutrient cycling, and subsequent competition, was unfortunately, not incorporated due to a lack of observational data. The NUCOM model was developed to assess the impact of climate change on bog ecosystems using 200-500 years simulations. For the first time, a version of the Peatland-VU model has been used to simulate multi decal changes. Running the model over longer time periods, for example, similar to the NUCOM's 1760–2000 simulation period, and validating against macrofossil evidence can better assess the model's ability to reproduce shifts in vegetation in response to environmental changes. Future works, could use forward or backward multi-century climate projections to further investigate PVN's ability to respond to climate change and make projections as to how climate change may impact peatland ecosystems, either for the Netherlands or elsewhere.

5 Conclusions

Peat-forming vegetation can reduce GHG emissions when rewetting. We showed that the PFT composition on teh ecosystem scale has the potential reduce simulated GHG emissions in restored peatlands. We showed that harvests also have the potential to reduce GHG emissions and that the extent of this impact is dependent on the initial plants. Harvest played a greater role on GHG and CO_2 emissions in scenarios incuding TYPHA PFT compositions than MOSS PFT compositions. Whilst, previous studies have investigated whether singular plant types impact peatland net GHG emissions, few (or no) studies have investigated the impact of dynamic plant composition (or re-establishing ecosystems) on GHG emissions. This question is particularly timely because there exists an urgent need to reduce land subsidence whilst achieving carbon sequestration in peatlands. These results showed that peatland restoration efforts that rewet without restoring peat-forming vegetation will likely result in larger GHG emissions than restoration efforts that rewet and abandon. These results indicate that vegetation re-establishment is a critical component of peatland restoration.

Code and data availability. PVN 1.0 source code is available at bitbucket.org/tlippmann/pvn_public (last access: 18 May 2022). All input data used to generate the model scenarios presented in this study can be accessed through this bitbucket. This includes site model parameterisations, site soil profiles, climate data, water table data, and PFTs. The exact version of the model source code used to produce the results presented in this paper is archived on Zenodo (https://doi.org/10.5281/zenodo.6802102, Lippmann (2022)).

https://doi.org/10.5194/gmd-2022-143
Preprint. Discussion started: 26 July 2022

Geoscientific Model Development Discussions

Author contributions. TL, KvH, and MH developed the theoretical framework of the model. TL performed the model developments, composed the PFTs, made the figures, all analyses, and wrote the paper. TL and KvH collected the observational data, and developed the model parameterisation scheme, and soil profiles. KvH pre-processed the observational data and offered valuable suggestions on the development and calibration of the model. HD participated in the writing of this paper. HD, MH, KvH,YvdV participated in the revision of this paper. DH, HD, MH, and KvH aquired the funding and administered this project.

Competing interests. The contact author has declared that neither they nor their co-authors have any competing interests.

Acknowledgements. We would like to thank the editor and the reviewers for their valuable comments and suggestions. We thank Merit van den Berg for proof-reading.

https://doi.org/10.5194/gmd-2022-143
Preprint. Discussion started: 26 July 2022

References

Alhoz, K., Kenesei, K., Papageorgiou, M., Keurentjes, E. E. M., and de Jong, M.: Improved AHN3 Gridded DTM/DSM, 2020.

Bardgett, R. D., Freeman, C., and Ostle, N. J.: Microbial contributions to climate change through carbon cycle feedbacks, ISME Journal, 2, 805–814, https://doi.org/10.1038/ismej.2008.58, 2008.

Bauer, I. E.: Modelling effects of litter quality and environment on peat accumulation over different time-scales, Journal of Ecology, 92, 661–674, https://doi.org/10.1111/j.0022-0477.2004.00905.x, 2004.

Bona, K. A., Shaw, C., Thompson, D. K., Hararuk, O., Webster, K., Zhang, G., Voicu, M., and Kurz, W. A.: The Canadian model for peatlands (CaMP): A peatland carbon model for national greenhouse gas reporting, Ecological Modelling, 431, 109 164, https://doi.org/10.1016/j.ecolmodel.2020.109164, https://doi.org/10.1016/j.ecolmodel.2020.109164, 2020.

Box, J. E., Colgan, W. T., Christensen, T. R., Schmidt, N. M., Lund, M., Parmentier, F. J. W., Brown, R., Bhatt, U. S., Euskirchen, E. S., Romanovsky, V. E., Walsh, J. E., Overland, J. E., Wang, M., Corell, R. W., Meier, W. N., Wouters, B., Mernild, S., Mård, J., Pawlak, J., and Olsen, M. S.: Key indicators of Arctic climate change: 1971-2017, Environmental Research Letters, 14, https://doi.org/10.1088/1748-9326/aafc1b, 2019.

Bridgham, S. D., Cadillo-Quiroz, H., Keller, J. K., and Zhuang, Q.: Methane emissions from wetlands: Biogeochemical, microbial, and modeling perspectives from local to global scales, Global Change Biology, 19, 1325–1346, https://doi.org/10.1111/gcb.12131, 2013.

Bustamante, M., Robledo-Abad, C., Harper, R., Mbow, C., Ravindranat, N. H., Sperling, F., Haberl, H., Pinto, A. d. S., and Smith, P.: Co-benefits, trade-offs, barriers and policies for greenhouse gas mitigation in the agriculture, forestry and other land use (AFOLU) sector, Global Change Biology, 20, 3270–3290, https://doi.org/10.1111/gcb.12591, 2014.

Chaudhary, N., Miller, P. A., and Smith, B.: Modelling Holocene peatland dynamics with an individual-based dynamic vegetation model, Biogeosciences, 14, 2571–2596, https://doi.org/10.5194/bg-14-2571-2017, 2017.

De Boeck, H. J., Dreesen, F. E., Janssens, I. a., and Nijs, I.: Whole-system responses of experimental plant communities to climate extremes imposed in different seasons., The New phytologist, 189, 806–17, https://doi.org/10.1111/j.1469-8137.2010.03515.x, http://www.ncbi.nlm.nih.gov/pubmed/21054412, 2011.

De Lange, W. J., Prinsen, G. F., Hoogewoud, J. C., Veldhuizen, A. A., Verkaik, J., Oude Essink, G. H. P., Van Walsum, P. E. V., Delsman, J. R., Hunink, J. C., Massop, H. T. L., and Kroon, T.: An operational, multi-scale, multi-model system for consensus-based, integrated water management and policy analysis: The Netherlands Hydrological Instrument., Environmental Modelling and Software, 59, 98–108, https://doi.org/10.1016/j.envsoft.2014.05.009, http://dx.doi.org/10.1016/j.envsoft.2014.05.009, 2014.

Doblas-Reyes, F. J., Sörensson, A. A., Almazroui, M., Dosio, A., Gutowski, W. J., Haarsma, R., Hamdi, R., Hewitson, B., Kwon, W.-T., Lamptey, B. L., Maraun, D., Stephenson, T. S., Takayabu, I., Terray, L., Turner, A., and Zuo, Z.: Linking Global to Regional Climate Change, in: Climate Change 2021: The Physical Science Basis. Contribution of Working Group I to the Sixth Assessment Report of the Intergovernmental Panel on Climate Change, edited by Masson-Delmotte, V., Zhai, P., Pirani, A., Connors, S. L., Péan, C., Berger, S., Caud, N., Chen, Y., Goldfarb, L., Gomis, M. I., Huang, M., Leitzell, K., Lonnoy, E., Matthews, J. B. R., Maycock, T. K., Waterfield, T., Yelekçi, O., Yu, R., and Zhou, B., chap. Linking Gl, pp. 1363–1512, Cambridge University Press, Cambridge, United Kingdom and New York, NY, USA, https://doi.org/10.1017/9781009157896.012, https://www.ipcc.ch/, 2021.

Dorrepaal, E., Aerts, R., Cornelissen, J. H., Van Logtestijn, R. S., and Callaghan, T. V.: Sphagnum modifies climate-change impacts on subarctic vascular bog plants, Functional Ecology, 20, 31–41, https://doi.org/10.1111/j.1365-2435.2006.01076.x, 2006.

https://doi.org/10.5194/gmd-2022-143
Preprint. Discussion started: 26 July 2022

Dorrepaal, E., Cornelissen, J. H., and Aerts, R.: Changing leaf litter feedbacks on plant production across contrasting sub-arctic peatland species and growth forms, Oecologia, 151, 251–261, https://doi.org/10.1007/s00442-006-0580-3, 2007.

Dorrepaal, E., Toet, S., Van Logtestijn, R. S., Swart, E., Van De Weg, M. J., Callaghan, T. V., and Aerts, R.: Carbon respiration from subsurface peat accelerated by climate warming in the subarctic, Nature, 460, 616–619, https://doi.org/10.1038/nature08216, http://dx.doi.org/10.1038/nature08216, 2009.

Erkens, G., van der Meulen, M. J., and Middelkoop, H.: Double trouble: subsidence and CO 2 respiration due to 1,000 years of Dutch coastal peatlands cultivation, Hydrogeology Journal, 24, 551–568, https://doi.org/10.1007/s10040-016-1380-4, 2016.

et al. Van Der Ree: Klimaatakkoord: effecten op veiligheid, gezondheid en natuur, pp. 59–61, https://www.rivm.nl/publicaties/klimaatakkoord-effecten-op-veiligheid-gezondheid-en-natuur#abstract_en, 2019.

Frolking, S. and Roulet, N. T.: Holocene radiative forcing impact of northern peatland carbon accumulation and methane emissions, Global Change Biology, 13, 1079–1088, https://doi.org/10.1111/j.1365-2486.2007.01339.x, 2007.

Frolking, S., Roulet, N. T., Tuittila, E., Bubier, J. L., Quillet, A., Talbot, J., and Richard, P. J. H.: A new model of Holocene peatland net primary production, decomposition, water balance, and peat accumulation, Earth System Dynamics, 1, 1–21, https://doi.org/10.5194/esd-1-1-2010, https://esd.copernicus.org/preprints/1/115/2010/https://esd.copernicus.org/articles/1/1/2010/, 2010.

García-Herrera, R., Garrido-Perez, J. M., Barriopedro, D., Ordóñez, C., Vicente-Serrano, S. M., Nieto, R., Gimeno, L., Sorí, R., and Yiou, P.: The European 2016/17 drought, Journal of Climate, 32, 3169–3187, https://doi.org/10.1175/JCLI-D-18-0331.1, 2019.

Geurts, J. and Fritz, C.: Paludiculture pilots and experiments with focus on cattail and reed in the Netherlands. Technical, Tech. rep., Radboud University Nijmegen, Nijmegen, https://repository.ubn.ru.nl/handle/2066/192628, 2018.

Gorham, E.: Northern Peatlands : Role in the Carbon Cycle and Probable Responses to Climatic Warming, Ecological Applications, 1, 182–195, https://doi.org/10.2307/1941811, 1991.

Günther, A., Huth, V., Jurasinski, G., and Glatzel, S.: The effect of biomass harvesting on greenhouse gas emissions from a rewetted temperate fen, GCB Bioenergy, pp. 1092–1106, https://doi.org/10.1111/gcbb.12214, 2014.

Günther, A., Barthelmes, A., Huth, V., Joosten, H., Jurasinski, G., Koebsch, F., and Couwenberg, J.: Prompt rewetting of drained peatlands reduces climate warming despite methane emissions, Nature Communications, 11, 1644, https://doi.org/10.1038/s41467-020-15499-z, http://www.nature.com/articles/s41467-020-15499-z, 2020.

Harpenslager, S. F., van den Elzen, E., Kox, M. A., Smolders, A. J., Ettwig, K. F., and Lamers, L. P.: Rewetting former agricultural peatlands: Topsoil removal as a prerequisite to avoid strong nutrient and greenhouse gas emissions, Ecological Engineering, 84, 159–168, https://doi.org/10.1016/j.ecoleng.2015.08.002, http://dx.doi.org/10.1016/j.ecoleng.2015.08.002, 2015.

Haxeltine, A., Prentice, I. C., and Creswell, I. D.: A coupled carbon and water flux model to predict vegetation structure, Journal of Vegetation Science, 7, 651–666, https://doi.org/10.2307/3236377, 1996.

Heijmans, M. and Berendse, F.: NUCOM: a dynamic vegetation model for peatlands and tundra including nitrogen cycling and mosses, 2008.

Heijmans, M. M. P. D., Mauquoy, D., Van Geel, B., and Berendse, F.: Long-term effects of climate change on vegetation and carbon dynamics in peat bogs, Journal of Vegetation Science, 19, 307–320, https://doi.org/10.3170/2008-8-18368, https://www.scopus.com/inward/record.url?eid=2-s2.0-41849115693&partnerID=40&md5=650f510b7f8fb783728dc3e00073b873, 2008.

Heinemeyer, A., Croft, S., Garnett, M. H., Gloor, E., Holden, J., Lomas, M. R., and Ineson, P.: The MILLENNIA peat cohort model: Predicting past, present and future soil carbon budgets and fluxes under changing climates in peatlands, Climate Research, 45, 207–226, https://doi.org/10.3354/cr00928, 2010.

https://doi.org/10.5194/gmd-2022-143
Preprint. Discussion started: 26 July 2022

Hendriks, D. M., Van Huissteden, J., Dolman, A. J., and Van Der Molen, M. K.: The full greenhouse gas balance of an abandoned peat meadow, Biogeosciences, 4, 411–424, https://doi.org/10.5194/bg-4-411-2007, 2007.

Hobbie, S. E., Schimel, J. P., Trumbore, S. E., and Randerson, J. R.: Controls over carbon storage and turnover in high-latitude soils, Global Change Biology, 6, 196–210, https://doi.org/10.1046/j.1365-2486.2000.06021.x, 2000.

Huang, S., Titus, S. J., and Wiens, D. P.: Comparison of nonlinear height-diameter functions for major Alberta tree species, Canadian Journal of Forest Research, 22, 1297–1304, https://doi.org/10.1139/x92-172, https://cdnsciencepub.com/doi/10.1139/x92-172http://www.nrcresearchpress.com/doi/10.1139/x92-172, 1992.

IPCC Working Group II: IPCC AR6 Working Group II: Summary for policymakers: Climate Change 2022, Impacts, Adaptation anf Vulnerability, in: Contribution of Working Group II to the Sixth Assessment Report of the Intergovernmental Panel on Climate Change, pp. xxiii–xxxiii, Cambridge University Press, 2022.

Iversen, C. M., Sloan, V. L., Sullivan, P. F., Euskirchen, E. S., McGuire, A. D., Norby, R. J., Walker, A. P., Warren, J. M., and Wullschleger, S. D.: The unseen iceberg: plant roots in arctic tundra, New Phytologist, 205, 34–58, https://doi.org/10.1111/nph.13003, http://www.ncbi.nlm.nih.gov/pubmed/25209220https://onlinelibrary.wiley.com/doi/10.1111/nph.13003, 2015.

Joosten, H.: The Global Peatland Carbon dioxide Picture, Quaternary Science Reviews, pp. 1–10, http://linkinghub.elsevier.com/retrieve/pii/S0277379111000333, 2010.

Kattge, J., Díaz, S., Lavorel, S., Prentice, I. C., Leadley, P., Bönisch, G., Garnier, E., Westoby, M., Reich, P. B., Wright, I. J., Cornelissen, J. H., Violle, C., Harrison, S. P., Van Bodegom, P. M., Reichstein, M., Enquist, B. J., Soudzilovskaia, N. A., Ackerly, D. D., Anand, M., Atkin, O., Bahn, M., Baker, T. R., Baldocchi, D., Bekker, R., Blanco, C. C., Blonder, B., Bond, W. J., Bradstock, R., Bunker, D. E., Casanoves, F., Cavender-Bares, J., Chambers, J. Q., Chapin, F. S., Chave, J., Coomes, D., Cornwell, W. K., Craine, J. M., Dobrin, B. H., Duarte, L., Durka, W., Elser, J., Esser, G., Estiarte, M., Fagan, W. F., Fang, J., Fernández-Méndez, F., Fidelis, A., Finegan, B., Flores, O., Ford, H., Frank, D., Freschet, G. T., Fyllas, N. M., Gallagher, R. V., Green, W. A., Gutierrez, A. G., Hickler, T., Higgins, S. I., Hodgson, J. G., Jalili, A., Jansen, S., Joly, C. A., Kerkhoff, A. J., Kirkup, D., Kitajima, K., Kleyer, M., Klotz, S., Knops, J. M., Kramer, K., Kühn, I., Kurokawa, H., Laughlin, D., Lee, T. D., Leishman, M., Lens, F., Lenz, T., Lewis, S. L., Lloyd, J., Llusià, J., Louault, F., Ma, S., Mahecha, M. D., Manning, P., Massad, T., Medlyn, B. E., Messier, J., Moles, A. T., Müller, S. C., Nadrowski, K., Naeem, S., Niinemets, Ü., Nöllert, S., Nüske, A., Ogaya, R., Oleksyn, J., Onipchenko, V. G., Onoda, Y., Ordoñez, J., Overbeck, G., Ozinga, W. A., Patiño, S., Paula, S., Pausas, J. G., Peñuelas, J., Phillips, O. L., Pillar, V., Poorter, H., Poorter, L., Poschlod, P., Prinzing, A., Proulx, R., Rammig, A., Reinsch, S., Reu, B., Sack, L., Salgado-Negret, B., Sardans, J., Shiodera, S., Shipley, B., Siefert, A., Sosinski, E., Soussana, J. F., Swaine, E., Swenson, N., Thompson, K., Thornton, P., Waldram, M., Weiher, E., White, M., White, S., Wright, S. J., Yguel, B., Zaehle, S., Zanne, A. E., and Wirth, C.: TRY - a global database of plant traits, Global Change Biology, 17, 2905–2935, https://doi.org/10.1111/j.1365-2486.2011.02451.x, 2011.

Kattge, J., Bönisch, G., Díaz, S., Lavorel, S., Prentice, I. C., Leadley, P., Tautenhahn, S., Werner, G. D., Aakala, T., Abedi, M., Acosta, A. T., Adamidis, G. C., Adamson, K., Aiba, M., Albert, C. H., Alcántara, J. M., Alcázar C, C., Aleixo, I., Ali, H., Amiaud, B., Ammer, C., Amoroso, M. M., Anand, M., Anderson, C., Anten, N., Antos, J., Apgaua, D. M. G., Ashman, T. L., Asmara, D. H., Asner, G. P., Aspinwall, M., Atkin, O., Aubin, I., Baastrup-Spohr, L., Bahalkeh, K., Bahn, M., Baker, T., Baker, W. J., Bakker, J. P., Baldocchi, D., Baltzer, J., Banerjee, A., Baranger, A., Barlow, J., Barneche, D. R., Baruch, Z., Bastianelli, D., Battles, J., Bauerle, W., Bauters, M., Bazzato, E., Beckmann, M., Beeckman, H., Beierkuhnlein, C., Bekker, R., Belfry, G., Belluau, M., Beloiu, M., Benavides, R., Benomar, L., Berdugo-Lattke, M. L., Berenguer, E., Bergamin, R., Bergmann, J., Bergmann Carlucci, M., Berner, L., Bernhardt-Römermann, M., Bigler, C., Bjorkman, A. D., Blackman, C., Blanco, C., Blonder, B., Blumenthal, D., Bocanegra-González, K. T., Boeckx, P., Bohlman, S.,

https://doi.org/10.5194/gmd-2022-143
Preprint. Discussion started: 26 July 2022

Böhning-Gaese, K., Boisvert-Marsh, L., Bond, W., Bond-Lamberty, B., Boom, A., Boonman, C. C., Bordin, K., Boughton, E. H., Boukili, V., Bowman, D. M., Bravo, S., Brendel, M. R., Broadley, M. R., Brown, K. A., Bruelheide, H., Brumnich, F., Bruun, H. H., Bruy, D., Buchanan, S. W., Bucher, S. F., Buchmann, N., Buitenwerf, R., Bunker, D. E., Bürger, J., Burrascano, S., Burslem, D. F., Butterfield, B. J., Byun, C., Marques, M., Scalon, M. C., Caccianiga, M., Cadotte, M., Cailleret, M., Camac, J., Camarero, J. J., Campany, C., Campetella, G., Campos, J. A., Cano-Arboleda, L., Canullo, R., Carbognani, M., Carvalho, F., Casanoves, F., Castagneyrol, B., Catford, J. A., Cavender-Bares, J., Cerabolini, B. E., Cervellini, M., Chacón-Madrigal, E., Chapin, K., Chapin, F. S., Chelli, S., Chen, S. C., Chen, A., Cherubini, P., Chianucci, F., Choat, B., Chung, K. S., Chytrý, M., Ciccarelli, D., Coll, L., Collins, C. G., Conti, L., Coomes, D., Cornelissen, J. H., Cornwell, W. K., Corona, P., Coyea, M., Craine, J., Craven, D., Cromsigt, J. P., Csecserits, A., Cufar, K., Cuntz, M., da Silva, A. C., Dahlin, K. M., Dainese, M., Dalke, I., Dalle Fratte, M., Dang-Le, A. T., Danihelka, J., Dannoura, M., Dawson, S., de Beer, A. J., De Frutos, A., De Long, J. R., Dechant, B., Delagrange, S., Delpierre, N., Derroire, G., Dias, A. S., Diaz-Toribio, M. H., Dimitrakopoulos, P. G., Dobrowolski, M., Doktor, D., Dřevojan, P., Dong, N., Dransfield, J., Dressler, S., Duarte, L., Ducouret, E., Dullinger, S., Durka, W., Duursma, R., Dymova, O., E-Vojtkó, A., Eckstein, R. L., Ejtehadi, H., Elser, J., Emilio, T., Engemann, K., Erfanian, M. B., Erfmeier, A., Esquivel-Muelbert, A., Esser, G., Estiarte, M., Domingues, T. F., Fagan, W. F., Fagúndez, J., Falster, D. S., Fan, Y., Fang, J., Farris, E., Fazlioglu, F., Feng, Y., Fernandez-Mendez, F., Ferrara, C., Ferreira, J., Fidelis, A., Finegan, B., Firn, J., Flowers, T. J., Flynn, D. F., Fontana, V., Forey, E., Forgiarini, C., François, L., Frangipani, M., Frank, D., Frenette-Dussault, C., Freschet, G. T., Fry, E. L., Fyllas, N. M., Mazzochini, G. G., Gachet, S., Gallagher, R., Ganade, G., Ganga, F., García-Palacios, P., Gargaglione, V., Garnier, E., Garrido, J. L., de Gasper, A. L., Gea-Izquierdo, G., Gibson, D., Gillison, A. N., Giroldo, A., Glasenhardt, M. C., Gleason, S., Gliesch, M., Goldberg, E., Göldel, B., Gonzalez-Akre, E., Gonzalez-Andujar, J. L., González-Melo, A., González-Robles, A., Graae, B. J., Granda, E., Graves, S., Green, W. A., Gregor, T., Gross, N., Guerin, G. R., Günther, A., Gutiérrez, A. G., Haddock, L., Haines, A., Hall, J., Hambuckers, A., Han, W., Harrison, S. P., Hattingh, W., Hawes, J. E., He, T., He, P., Heberling, J. M., Helm, A., Hempel, S., Hentschel, J., Hérault, B., Hereş, A. M., Herz, K., Heuertz, M., Hickler, T., Hietz, P., Higuchi, P., Hipp, A. L., Hirons, A., Hock, M., Hogan, J. A., Holl, K., Honnay, O., Hornstein, D., Hou, E., Hough-Snee, N., Hovstad, K. A., Ichie, T., Igić, B., Illa, E., Isaac, M., Ishihara, M., Ivanov, L., Ivanova, L., Iversen, C. M., Izquierdo, J., Jackson, R. B., Jackson, B., Jactel, H., Jagodzinski, A. M., Jandt, U., Jansen, S., Jenkins, T., Jentsch, A., Jespersen, J. R. P., Jiang, G. F., Johansen, J. L., Johnson, D., Jokela, E. J., Joly, C. A., Jordan, G. J., Joseph, G. S., Junaedi, D., Junker, R. R., Justes, E., Kabzems, R., Kane, J., Kaplan, Z., Kattenborn, T., Kavelenova, L., Kearsley, E., Kempel, A., Kenzo, T., Kerkhoff, A., Khalil, M. I., Kinlock, N. L., Kissling, W. D., Kitajima, K., Kitzberger, T., Kjøller, R., Klein, T., Kleyer, M., Klimešová, J., Klipel, J., Kloeppel, B., Klotz, S., Knops, J. M., Kohyama, T., Koike, F., Kollmann, J., Komac, B., Komatsu, K., König, C., Kraft, N. J., Kramer, K., Kreft, H., Kühn, I., Kumarathunge, D., Kuppler, J., Kurokawa, H., Kurosawa, Y., Kuyah, S., Laclau, J. P., Lafleur, B., Lallai, E., Lamb, E., Lamprecht, A., Larkin, D. J., Laughlin, D., Le Bagousse-Pinguet, Y., le Maire, G., le Roux, P. C., le Roux, E., Lee, T., Lens, F., Lewis, S. L., Lhotsky, B., Li, Y., Li, X., Lichstein, J. W., Liebergesell, M., Lim, J. Y., Lin, Y. S., Linares, J. C., Liu, C., Liu, D., Liu, U., Livingstone, S., Llusià, J., Lohbeck, M., López-García, Á., Lopez-Gonzalez, G., Lososová, Z., Louault, F., Lukács, B. A., Lukeš, P., Luo, Y., Lussu, M., Ma, S., Maciel Rabelo Pereira, C., Mack, M., Maire, V., Mäkelä, A., Mäkinen, H., Malhado, A. C. M., Mallik, A., Manning, P., Manzoni, S., Marchetti, Z., Marchino, L., Marcilio-Silva, V., Marcon, E., Marignani, M., Markesteijn, L., Martin, A., Martínez-Garza, C., Martínez-Vilalta, J., Mašková, T., Mason, K., Mason, N., Massad, T. J., Masse, J., Mayrose, I., McCarthy, J., McCormack, M. L., McCulloh, K., McFadden, I. R., McGill, B. J., McPartland, M. Y., Medeiros, J. S., Medlyn, B., Meerts, P., Mehrabi, Z., Meir, P., Melo, F. P., Mencuccini, M., Meredieu, C., Messier, J., Mészáros, I., Metsaranta, J., Michaletz, S. T., Michelaki, C., Migalina, S., Milla, R., Miller, J. E., Minden, V., Ming, R., Mokany, K., Moles, A. T., Molnár, A., Molofsky, J., Molz, M., Montgomery, R. A., Monty, A., Moravcová, L., Moreno-Martínez, A., Moretti, M., Mori, A. S., Mori, S., Morris, D., Morrison, J., Mucina, L., Mueller, S., Muir, C. D.,

https://doi.org/10.5194/gmd-2022-143
Preprint. Discussion started: 26 July 2022

Müller, S. C., Munoz, F., Myers-Smith, I. H., Myster, R. W., Nagano, M., Naidu, S., Narayanan, A., Natesan, B., Negoita, L., Nelson, A. S., Neuschulz, E. L., Ni, J., Niedrist, G., Nieto, J., Niinemets, Ü., Nolan, R., Nottebrock, H., Nouvellon, Y., Novakovskiy, A., Nystuen, K. O., O'Grady, A., O'Hara, K., O'Reilly-Nugent, A., Oakley, S., Oberhuber, W., Ohtsuka, T., Oliveira, R., Öllerer, K., Olson, M. E., Onipchenko, V., Onoda, Y., Onstein, R. E., Ordonez, J. C., Osada, N., Ostonen, I., Ottaviani, G., Otto, S., Overbeck, G. E., Ozinga, W. A., Pahl, A. T., Paine, C. E., Pakeman, R. J., Papageorgiou, A. C., Parfionova, E., Pärtel, M., Patacca, M., Paula, S., Paule, J., Pauli, H., Pausas, J. G., Peco, B., Penuelas, J., Perea, A., Peri, P. L., Petisco-Souza, A. C., Petraglia, A., Petritan, A. M., Phillips, O. L., Pierce, S., Pillar, V. D., Pisek, J., Pomogaybin, A., Poorter, H., Portsmuth, A., Poschlod, P., Potvin, C., Pounds, D., Powell, A. S., Power, S. A., Prinzing, A., Puglielli, G., Pyšek, P., Raevel, V., Rammig, A., Ransijn, J., Ray, C. A., Reich, P. B., Reichstein, M., Reid, D. E., Réjou-Méchain, M., de Dios, V. R., Ribeiro, S., Richardson, S., Riibak, K., Rillig, M. C., Riviera, F., Robert, E. M., Roberts, S., Robroek, B., Roddy, A., Rodrigues, A. V., Rogers, A., Rollinson, E., Rolo, V., Römermann, C., Ronzhina, D., Roscher, C., Rosell, J. A., Rosenfield, M. F., Rossi, C., Roy, D. B., Royer-Tardif, S., Rüger, N., Ruiz-Peinado, R., Rumpf, S. B., Rusch, G. M., Ryo, M., Sack, L., Saldaña, A., Salgado-Negret, B., Salguero-Gomez, R., Santa-Regina, I., Santacruz-García, A. C., Santos, J., Sardans, J., Schamp, B., Scherer-Lorenzen, M., Schleuning, M., Schmid, B., Schmidt, M., Schmitt, S., Schneider, J. V., Schowanek, S. D., Schrader, J., Schrodt, F., Schuldt, B., Schurr, F., Selaya Garvizu, G., Semchenko, M., Seymour, C., Sfair, J. C., Sharpe, J. M., Sheppard, C. S., Sheremetiev, S., Shiodera, S., Shipley, B., Shovon, T. A., Siebenkäs, A., Sierra, C., Silva, V., Silva, M., Sitzia, T., Sjöman, H., Slot, M., Smith, N. G., Sodhi, D., Soltis, P., Soltis, D., Somers, B., Sonnier, G., Sørensen, M. V., Sosinski, E. E., Soudzilovskaia, N. A., Souza, A. F., Spasojevic, M., Sperandii, M. G., Stan, A. B., Stegen, J., Steinbauer, K., Stephan, J. G., Sterck, F., Stojanovic, D. B., Strydom, T., Suarez, M. L., Svenning, J. C., Svitková, I., Svitok, M., Svoboda, M., Swaine, E., Swenson, N., Tabarelli, M., Takagi, K., Tappeiner, U., Tarifa, R., Tauugourdeau, S., Tavsanoglu, C., te Beest, M., Tedersoo, L., Thiffault, N., Thom, D., Thomas, E., Thompson, K., Thornton, P. E., Thuiller, W., Tichý, L., Tissue, D., Tjoelker, M. G., Tng, D. Y. P., Tobias, J., Török, P., Tarin, T., Torres-Ruiz, J. M., Tóthmérész, B., Treurnicht, M., Trivellone, V., Trolliet, F., Trotsiuk, V., Tsakalos, J. L., Tsiripidis, I., Tysklind, N., Umehara, T., Usoltsev, V., Vadeboncoeur, M., Vaezi, J., Valladares, F., Vamosi, J., van Bodegom, P. M., van Breugel, M., Van Cleemput, E., van de Weg, M., van der Merwe, S., van der Plas, F., van der Sande, M. T., van Kleunen, M., Van Meerbeek, K., Vanderwel, M., Vanselow, K. A., Vårhammar, A., Varone, L., Vasquez Valderrama, M. Y., Vassilev, K., Vellend, M., Veneklaas, E. J., Verbeeck, H., Verheyen, K., Vibrans, A., Vieira, I., Villacís, J., Violle, C., Vivek, P., Wagner, K., Waldram, M., Waldron, A., Walker, A. P., Waller, M., Walther, G., Wang, H., Wang, F., Wang, W., Watkins, H., Watkins, J., Weber, U., Weedon, J. T., Wei, L., Weigelt, P., Weiher, E., Wells, A. W., Wellstein, C., Wenk, E., Westoby, M., Westwood, A., White, P. J., Whitten, M., Williams, M., Winkler, D. E., Winter, K., Womack, C., Wright, I. J., Wright, S. J., Wright, J., Pinho, B. X., Ximenes, F., Yamada, T., Yamaji, K., Yanai, R., Yankov, N., Yguel, B., Zanini, K. J., Zanne, A. E., Zelený, D., Zhao, Y. P., Zheng, J., Zheng, J., Ziemińska, K., Zirbel, C. R., Zizka, G., Zo-Bi, I. C., Zotz, G., and Wirth, C.: TRY plant trait database – enhanced coverage and open access, Global Change Biology, 26, 119–188, https://doi.org/10.1111/gcb.14904, 2020.

Knox, S. H., Sturtevant, C., Matthes, J. H., Koteen, L., Verfaillie, J., and Baldocchi, D.: Agricultural peatland restoration: Effects of land-use change on greenhouse gas (CO2and CH4) fluxes in the Sacramento-San Joaquin Delta, Global Change Biology, 21, 750–765, https://doi.org/10.1111/gcb.12745, 2015.

Krinner, G., Viovy, N., de Noblet-Ducoudré, N., Ogée, J., Polcher, J., Friedlingstein, P., Ciais, P., Sitch, S., and Prentice, I. C.: A dynamic global vegetation model for studies of the coupled atmosphere-biosphere system, Global Biogeochemical Cycles, 19, 1–33, https://doi.org/10.1029/2003GB002199, http://doi.wiley.com/10.1029/2003GB002199, 2005.

Lafleur, P. M., Roulet, N. T., Bubier, J. L., Frolking, S., and Moore, T. R.: Interannual variability in the peatland-atmosphere carbon dioxide exchange at an ombrotrophic bog, Global Biogeochemical Cycles, 17, 1–14, https://doi.org/10.1029/2002gb001983, 2003.

https://doi.org/10.5194/gmd-2022-143
Preprint. Discussion started: 26 July 2022

Largeron, C., Krinner, G., Ciais, P., and Brutel-Vuilmet, C.: Implementing northern peatlands in a global land surface model: Description and evaluation in the ORCHIDEE high-latitude version model (ORC-HL-PEAT), Geoscientific Model Development, 11, 3279–3297, https://doi.org/10.5194/gmd-11-3279-2018, 2018.

Li, T., Raivonen, M., Alekseychik, P., Aurela, M., Lohila, A., Zheng, X., Zhang, Q., Wang, G., Mammarella, I., Rinne, J., Yu, L., Xie, B., Vesala, T., and Zhang, W.: Importance of vegetation classes in modeling CH4 emissions from boreal and subarctic wetlands in Finland, Science of the Total Environment, 572, 1111–1122, https://doi.org/10.1016/j.scitotenv.2016.08.020, http://dx.doi.org/10.1016/j.scitotenv.2016.08.020, 2016.

Lippmann, T. J. R.: PVN model (peatland GHG emissions model including plant functional types), https://doi.org/10.5281/zenodo.6802102, https://doi.org/10.5281/zenodo.6802102, 2022.

Littleton, E. W., Harper, A. B., Vaughan, N. E., Oliver, R. J., Duran-Rojas, M. C., and Lenton, T. M.: JULES-BE: representation of bioenergy crops and harvesting in the Joint UK Land Environment Simulator vn5.1, Geoscientific Model Development, 13, 1123–1136, https://doi.org/10.5194/gmd-13-1123-2020, https://gmd.copernicus.org/articles/13/1123/2020/, 2020.

Loisel, J., Gallego-Sala, A. V., Amesbury, M. J., Magnan, G., Anshari, G., Beilman, D. W., Benavides, J. C., Blewett, J., Camill, P., Charman, D. J., Chawchai, S., Hedgpeth, A., Kleinen, T., Korhola, A., Large, D., Mansilla, C. A., Müller, J., van Bellen, S., West, J. B., Yu, Z., Bubier, J. L., Garneau, M., Moore, T., Sannel, A. B., Page, S., Väliranta, M., Bechtold, M., Brovkin, V., Cole, L. E., Chanton, J. P., Christensen, T. R., Davies, M. A., De Vleeschouwer, F., Finkelstein, S. A., Frolking, S., Gałka, M., Gandois, L., Girkin, N., Harris, L. I., Heinemeyer, A., Hoyt, A. M., Jones, M. C., Joos, F., Juutinen, S., Kaiser, K., Lacourse, T., Lamentowicz, M., Larmola, T., Leifeld, J., Lohila, A., Milner, A. M., Minkkinen, K., Moss, P., Naafs, B. D., Nichols, J., O'Donnell, J., Payne, R., Philben, M., Piilo, S., Quillet, A., Ratnayake, A. S., Roland, T. P., Sjögersten, S., Sonnentag, O., Swindles, G. T., Swinnen, W., Talbot, J., Treat, C., Valach, A. C., and Wu, J.: Expert assessment of future vulnerability of the global peatland carbon sink, Nature Climate Change, 11, 70–77, https://doi.org/10.1038/s41558-020-00944-0, 2021.

Long, K. D., Flanagan, L. B., and Cai, T.: Diurnal and seasonal variation in methane emissions in a northern Canadian peatland measured by eddy covariance, Global Change Biology, 16, 2420–2435, https://doi.org/10.1111/j.1365-2486.2009.02083.x, 2010.

Melillo, J. M., Steudler, P. A., Aber, J. D., Newkirk, K., Lux, H., Bowles, F. P., Catricala, C., Magill, A., Ahrens, T., and Morrisseau, S.: Soil warming and carbon-cycle feedbacks to the climate system, Science, 298, 2173–2176, https://doi.org/10.1126/science.1074153, 2002.

Melton, J. R., Wania, R., Hodson, E. L., Poulter, B., Ringeval, B., Spahni, R., Bohn, T., Avis, C. A., Beerling, D. J., Chen, G., Eliseev, A. V., Denisov, S. N., Hopcroft, P. O., Lettenmaier, D. P., Riley, W. J., Singarayer, J. S., Subin, Z. M., Tian, H., Zürcher, S., Brovkin, V., van Bodegom, P. M., Kleinen, T., Yu, Z. C., and Kaplan, J. O.: Present state of global wetland extent and wetland methane modelling: conclusions from a model inter-comparison project (WETCHIMP), Biogeosciences, 10, 753–788, https://doi.org/10.5194/bg-10-753-2013, https://bg.copernicus.org/articles/10/753/2013/, 2013.

Metzger, C., Jansson, P. E., Lohila, A., Aurela, M., Eickenscheidt, T., Belelli-Marchesini, L., Dinsmore, K. J., Drewer, J., Van Huissteden, J., and Drösler, M.: CO2 fluxes and ecosystem dynamics at five European treeless peatlands-merging data and process oriented modeling, Biogeosciences, 12, 125–146, https://doi.org/10.5194/bg-12-125-2015, http://www.biogeosciences.net/12/125/2015/https://bg.copernicus.org/articles/12/125/2015/, 2015.

Mi, Y., Van Huissteden, J., Parmentier, F. J. W., Gallagher, A., Budishchev, A., Berridge, C. T., and Dolman, A. J.: Improving a plot-scale methane emission model and its performance at a northeastern Siberian tundra site, Biogeosciences, 11, 3985–3999, https://doi.org/10.5194/bg-11-3985-2014, 2014.

https://doi.org/10.5194/gmd-2022-143
Preprint. Discussion started: 26 July 2022

Müller, J. and Joos, F.: Global peatland area and carbon dynamics from the Last Glacial Maximum to the present – a process-based model investigation, Biogeosciences, 17, 5285–5308, https://doi.org/10.5194/bg-17-5285-2020, https://bg.copernicus.org/articles/17/5285/2020/, 2020.

Olefeldt, D., Turetsky, M. R., Crill, P. M., and Mcguire, A. D.: Environmental and physical controls on northern terrestrial methane emissions across permafrost zones, Global Change Biology, 19, 589–603, https://doi.org/10.1111/gcb.12071, 2013.

Paudel, R., Mahowald, N. M., Hess, P. G., Meng, L., and Riley, W. J.: Attribution of changes in global wetland methane emissions from pre-industrial to present using CLM4.5-BGC, Environmental Research Letters, 11, 034 020, https://doi.org/10.1088/1748-9326/11/3/034020, http://www.scopus.com/inward/record.url?eid=2-s2.0-84962270331&partnerID=tZOtx3y1, 2016.

Pavelka, M., Acosta, M., Kiese, R., Altimir, N., Brümmer, C., Crill, P., Darenova, E., Fuß, R., Gielen, B., Graf, A., Klemedtsson, L., Lohila, A., Longdoz, B., Lindroth, A., Nilsson, M., Jiménez, S. M., Merbold, L., Montagnani, L., Peichl, M., Pihlatie, M., Pumpanen, J., Ortiz, P. S., Silvennoinen, H., Skiba, U., Vestin, P., Weslien, P., Janous, D., and Kutsch, W.: Standardisation of chamber technique for CO 2 , N 2 O and CH 4 fluxes measurements from terrestrial ecosystems, International Agrophysics, 32, 569–587, https://doi.org/10.1515/intag-2017-0045, 2018.

Philippot, L., Hallin, S., Börjesson, G., and Baggs, E. M.: Biochemical cycling in the rhizosphere having an impact on global change, Plant and Soil, 321, 61–81, https://doi.org/10.1007/s11104-008-9796-9, https://www.jstor.org/stable/24130107, 2009.

Ringeval, B., De Noblet-Ducoudré, N., Ciais, P., Bousquet, P., Prigent, C., Papa, F., and Rossow, W. B.: An attempt to quantify the impact of changes in wetland extent on methane emissions on the seasonal and interannual time scales, Global Biogeochemical Cycles, 24, 1–12, https://doi.org/10.1029/2008GB003354, 2010.

Saleska, S. R., Shaw, M. R., Fischer, M. L., Dunne, J. A., Still, C. J., Holman, M. L., and Harte, J.: Plant community composition mediates both large transient decline and predicted long-term recovery of soil carbon under climate warming, Global Biogeochemical Cycles, 16, 3–1–3–18, https://doi.org/10.1029/2001gb001573, 2002.

Saunois, M., Stavert, A., Poulter, B., Bousquet, P., Canadell, J., Jackson, R., Raymond, P., Dlugokencky, E., Houweling, S., Patra, P., Ciais, P., Arora, V., Bastviken, D., Bergamaschi, P., Blake, D., Brailsford, G., Bruhwiler, L., Carlson, K., Carrol, M., Castaldi, S., Chandra, N., Crevoisier, C., Crill, P., Covey, K., Curry, C., Etiope, G., Frankenberg, C., Gedney, N., Hegglin, M., Höglund-Isaksson, L., Hugelius, G., Ishizawa, M., Ito, A., Janssens-Maenhout, G., Jensen, K., Joos, F., Kleinen, T., Krummel, P., Langenfelds, R., Laruelle, G., Liu, L., Machida, T., Maksyutov, S., McDonald, K., McNorton, J., Miller, P., Melton, J., Morino, I., Müller, J., Murguia-Flores, F., Naik, V., Niwa, Y., Noce, S., O'Doherty, S., Parker, R., Peng, C., Peng, S., Peters, G., Prigent, C., Prinn, R., Ramonet, M., Regnier, P., Riley, W., Rosentreter, J., Segers, A., Simpson, I., Shi, H., Smith, S., Steele, L. P., Thornton, B., Tian, H., Tohjima, Y., Tubiello, F., Tsuruta, A., Viovy, N., Voulgarakis, A., Weber, T., van Weele, M., van der Werf, G., Weiss, R., Worthy, D., Wunch, D., Yin, Y., Yoshida, Y., Zhang, W., Zhang, Z., Zhao, Y., Zheng, B., Zhu, Q., Zhu, Q., and Zhuang, Q.: The Global Methane Budget 2000–2017, Earth System Science Data, 12, 1561–1623, https://doi.org/10.5194/essd-12-1561-2020, 2020.

Schrier-Uijl, A. P., Kroon, P. S., Hendriks, D. M. D., Hensen, A., Huissteden, J. V., Berendse, F., and Veenendaal, E. M.: Agricultural peatlands : towards a greenhouse gas sink – a synthesis of a Dutch landscape study, Biogeosciences, 11, 4559–4576, https://doi.org/10.5194/bg-11-4559-2014, www.biogeosciences.net/11/4559/2014/, 2014.

Shi, X., Thornton, P. E., Ricciuto, D. M., Hanson, P. J., Mao, J., Sebestyen, S. D., Griffiths, N. A., and Bisht, G.: Representing northern peatland microtopography and hydrology within the Community Land Model, Biogeosciences, 12, 6463–6477, https://doi.org/10.5194/bg-12-6463-2015, www.biogeosciences.net/12/6463/2015/, 2015.

https://doi.org/10.5194/gmd-2022-143
Preprint. Discussion started: 26 July 2022

Sitch, S., Smith, B., Prentice, I. C., Arneth, A., Bondeau, A., Cramer, W., Kaplan, J. O., Levis, S., Lucht, W., Sykes, M. T., Thonicke, K., and Venevsky, S.: Evaluation of ecosystem dynamics, plant geography and terrestrial carbon cycling in the LPJ dynamic global vegetation model, Global Change Biology, 9, 161–185, https://doi.org/10.1046/j.1365-2486.2003.00569.x, 2003.

Smith, B., Prentice, I. C., and Sykes, M. T.: Representation of vegetation dynamics in the modelling of terrestrial ecosystems: comparing two contrasting approaches within European climate space, Global Ecology and Biogeography, 10, 621–637, https://doi.org/10.1046/j.1466-822x.2001.t01-1-00256.x, 2001.

Solomon, S., Manning, M., Marquis, M., Qin, D., and Others: Climate change 2007-the physical science basis: Working group I contribution to the fourth assessment report of the IPCC, vol. 4, Cambridge University Press, 2007.

Spahni, R., Wania, R., Neef, L., Van Weele, M., Pison, I., Bousquet, P., Frankenberg, C., Foster, P. N., Joos, F., Prentice, I. C., and Van Velthoven, P.: Constraining global methane emissions and uptake by ecosystems, Biogeosciences, 8, 1643–1665, https://doi.org/10.5194/bg-8-1643-2011, 2011.

Stocker, B. D., Spahni, R., and Joos, F.: DYPTOP: A cost-efficient TOPMODEL implementation to simulate sub-grid spatio-temporal dynamics of global wetlands and peatlands, Geoscientific Model Development, 7, 3089–3110, https://doi.org/10.5194/gmd-7-3089-2014, 2014.

Ström, L., Mastepanov, M., and Christensen, T. R.: Species-specific Effects of Vascular Plants on Carbon Turnover and Methane Emissions from Wetlands, Biogeochemistry, 75, 65–82, https://doi.org/10.1007/s10533-004-6124-1, https://doi.org/10.1007/s10533-004-6124-1http://link.springer.com/10.1007/s10533-004-6124-1, 2005.

Toet, S., Cornelissen, J. H., Aerts, R., Van Logtestijn, R. S., De Beus, M., and Stoevelaar, R.: Moss responses to elevated CO2 and variation in hydrology in a temperate lowland peatland, Plant Ecology, 182, 27–40, https://doi.org/10.1007/s11258-005-9029-8, 2006.

Törnqvist, L., Vartia, P., and Vartia, Y. O.: How Should Relative Changes be Measured?, The American Statistician, 39, 43–46, https://doi.org/10.1080/00031305.1985.10479385, https://doi.org/10.1080/00031305.1985.10479385, 1985.

Van den Hoof, C., Hanert, E., and Vidale, P. L.: Simulating dynamic crop growth with an adapted land surface model – JULES-SUCROS: Model development and validation, Agricultural and Forest Meteorology, 151, 137–153, https://doi.org/10.1016/j.agrformet.2010.09.011, https://linkinghub.elsevier.com/retrieve/pii/S0168192310002571, 2011.

van Geel, B., Bos, J. M., and Pals, J. P.: Archaeological and palaeoecological aspects of a medieval house terp in a reclaimed raiseg bog area in North Holland, Ber. Rijksd. Oudheidkd. Bodemonderz, 33, 419–444, 1983.

van Huissteden, J., van den Bos, R., and Alvarez, I. M.: Modeling the effect of water-table management on CO2 and CH4 fluxes from peat soils, Netherlands Journal of Geosciences, 85, 3–18, 2006.

van Huissteden, J., Petrescu, a. M. R., Hendriks, D. M. D., and Rebel, K. T.: Sensitivity analysis of a wetland methane emission model based on temperate and Arctic wetland sites, Biogeosciences, 6, 9083–9126, https://doi.org/10.5194/bgd-6-9083-2009, 2009.

Walter, B. P., Heimann, M., and Matthews, E.: Modeling modern methane emissions from natural wetlands, Journal of Geophysical Research Atmospheres, 106, 34 207–34 219, https://doi.org/10.1029/2001JD900164, 2001.

Walter, P. and Heimann, M.: A process-based, climate-sensitive model to derive methane emissions from natural wetlands: Application to five wetland sites, sensitivity to model parameters, and climate, Global Biogeochemical Cycles, 14, 745–765, 2000.

Wania, R., Ross, I., and Prentice, I. C.: Integrating peatlands and permafrost into a dynamic global vegetation model: 1. Evaluation and sensitivity of physical land surface processes, Global Biogeochemical Cycles, 23, n/a–n/a, https://doi.org/10.1029/2008GB003412, http://dx.doi.org/10.1029/2008GB003412http://doi.wiley.com/10.1029/2008GB003412, 2009.

https://doi.org/10.5194/gmd-2022-143
Preprint. Discussion started: 26 July 2022

Wania, R., Ross, I., and Prentice, I. C.: Implementation and evaluation of a new methane model within a dynamic global vegetation model: LPJ-WHyMe v1.3.1, Geoscientific Model Development, 3, 565–584, https://doi.org/10.5194/gmd-3-565-2010, 2010.

Wania, R., Melton, J. R., Hodson, E. L., Poulter, B., Ringeval, B., Spahni, R., Bohn, T., Avis, C. A., Chen, G., Eliseev, A. V., Hopcroft, P. O., Riley, W. J., Subin, Z. M., Tian, H., Van Bodegom, P. M., Kleinen, T., Yu, Z. C., Singarayer, J. S., Z??rcher, S., Lettenmaier, D. P., Beerling, D. J., Denisov, S. N., Prigent, C., Papa, F., and Kaplan, J. O.: Present state of global wetland extent and wetland methane modelling: Methodology of a model inter-comparison project (WETCHIMP), Geoscientific Model Development, 6, 617–641, https://doi.org/10.5194/gmd-6-617-2013, 2013.

Wu, J., Roulet, N. T., Moore, T. R., Lafleur, P., and Humphreys, E.: Dealing with microtopography of an ombrotrophic bog for simulating ecosystem-level CO2 exchanges, Ecological Modelling, 222, 1038–1047, https://doi.org/10.1016/j.ecolmodel.2010.07.015, http://dx.doi.org/10.1016/j.ecolmodel.2010.07.015, 2011.

Wu, Y. and Blodau, C.: PEATBOG: a biogeochemical model for analyzing coupled carbon and nitrogen dynamics in northern peatlands, Geoscientific Model Development, 6, 1173–1207, https://doi.org/10.5194/gmd-6-1173-2013, https://gmd.copernicus.org/articles/6/1173/2013/, 2013.

Wu, Y., Verseghy, D. L., and Melton, J. R.: Integrating peatlands into the coupled Canadian Land Surface Scheme (CLASS) v3.6 and the Canadian Terrestrial Ecosystem Model (CTEM) v2.0, Geoscientific Model Development, 9, 2639–2663, https://doi.org/10.5194/gmd-9-2639-2016, https://gmd.copernicus.org/articles/9/2639/2016/, 2016.

Wullschleger, S. D., Epstein, H. E., Box, E. O., Euskirchen, E. S., Goswami, S., Iversen, C. M., Kattge, J., Norby, R. J., van Bodegom, P. M., and Xu, X.: Plant functional types in Earth system models: past experiences and future directions for application of dynamic vegetation models in high-latitude ecosystems, Annals of Botany, 114, 1–16, https://doi.org/10.1093/aob/mcu077, https://academic.oup.com/aob/article-lookup/doi/10.1093/aob/mcu077, 2014.

Yu, Z., Loisel, J., Brosseau, D. P., Beilman, D. W., and Hunt, S. J.: Global peatland dynamics since the Last Glacial Maximum, Geophysical Research Letters, 37, 1–5, https://doi.org/10.1029/2010GL043584, 2010.

Yurova, A., Wolf, A., Sagerfors, J., and Nilsson, M.: Variations in net ecosystem exchange of carbon dioxide in a boreal mire: Modeling mechanisms linked to water table position, Journal of Geophysical Research, 112, G02 025, https://doi.org/10.1029/2006JG000342, http://doi.wiley.com/10.1029/2006JG000342, 2007.